Ecohydrological responses of dense canopies to environmental variability:
1. Interplay between vertical structure and photosynthetic pathway

D. T. Drewry,[1,2] P. Kumar,[1] S. Long,[3,4] C. Bernacchi,[4,5] X.-Z. Liang,[6,7] and M. Sivapalan[1,8]

Received 1 March 2010; revised 15 July 2010; accepted 7 September 2010; published 11 November 2010.

[1] Vegetation acclimation to changing climate, in particular elevated atmospheric concentrations of carbon dioxide (CO_2), has been observed to include modifications to the biochemical and ecophysiological functioning of leaves and the structural components of the canopy. These responses have the potential to significantly modify plant carbon uptake and surface energy partitioning, and have been attributed with large-scale changes in surface hydrology over recent decades. While the aggregated effects of vegetation acclimation can be pronounced, they often result from subtle changes in canopy properties that require the resolution of physical, biochemical and ecophysiological processes through the canopy for accurate estimation. In this paper, the first of two, a multilayer canopy-soil-root system model developed to capture the emergent vegetation responses to environmental change is presented. The model incorporates both C3 and C4 photosynthetic pathways, and resolves the vertical radiation, thermal, and environmental regimes within the canopy. The tight coupling between leaf ecophysiological functioning and energy balance determines vegetation responses to climate states and perturbations, which are modulated by soil moisture states through the depth of the root system. The model is validated for three growing seasons each for soybean (C3) and maize (C4) using eddy-covariance fluxes of CO_2, latent, and sensible heat collected at the Bondville (Illinois) Ameriflux tower site. The data set provides an opportunity to examine the role of important environmental drivers and model skill in capturing variability in canopy-atmosphere exchange. Vertical variation in radiative states and scalar fluxes over a mean diurnal cycle are examined to understand the role of canopy structure on the patterns of absorbed radiation and scalar flux magnitudes and the consequent differences in sunlit and shaded source/sink locations through the canopies. An analysis is made of the impact of soil moisture stress on carbon uptake and energy flux partitioning at the canopy-scale and resolved through the canopy, providing insight into the roles of canopy structure and metabolic pathway on the response of each crop to moisture deficits. Model calculations indicate increases in water use efficiency (*WUE*) with increasing moisture stress, with average maize *WUE* increases of 45% at the highest levels of plant stress examined here, relative to 20% increases for soybean.

Citation: Drewry, D. T., P. Kumar, S. Long, C. Bernacchi, X.-Z. Liang, and M. Sivapalan (2010), Ecohydrological responses of dense canopies to environmental variability: 1. Interplay between vertical structure and photosynthetic pathway, *J. Geophys. Res.*, *115*, G04022, doi:10.1029/2010JG001340.

1. Introduction

[2] The acclimation response of vegetation to changing climate, particularly to elevated CO_2 in the atmosphere, is now well documented [*Sage et al.*, 1989; *Curtis*, 1996;

[1]Department of Civil and Environmental Engineering, University of Illinois, Urbana, Illinois, USA.
[2]Now at Max Planck Institute for Biogeochemistry, Jena, Germany.
[3]Department of Crop Sciences, University of Illinois, Urbana, Illinois, USA.
[4]Department of Plant Biology, University of Illinois, Urbana, Illinois, USA.
[5]Global Change and Photosynthesis Research Unit, U.S. Department of Agriculture, Urbana, Illinois, USA.
[6]Department of Atmospheric Sciences, University of Illinois, Urbana, Illinois, USA.
[7]Illinois State Water Survey, Champaign, Illinois, USA.
[8]Department of Geography, University of Illinois, Urbana, Illinois, USA.

0148-0227/10/2010JG001340

Ainsworth and Long, 2005; *Gutschick*, 2007]. This response results in changes in structural characteristics, such as increased biomass in certain species [*Morgan et al.*, 2005; *Ainsworth and Long*, 2005; *Dermody et al.*, 2006], elevated leaf temperatures due to stomatal closure [*Sage*, 1994; *Curtis*, 1996; *Long et al.*, 2004], and shifts in biochemical response [*Huxman et al.*, 1998; *Long et al.*, 2004; *Bernacchi et al.*, 2005a]. These changes have been attributed with changes in streamflow [*Labat et al.*, 2004; *Gedney et al.*, 2006] suggesting large-scale impacts arising from these subtle but measureable responses. The goal of this study is to develop and validate a multilayer model that incorporates essential interactions of the structural, ecophysiological and biochemical functioning of the canopy that determine vegetation response to environmental perturbations. In the companion paper, the model is used to examine several emergent ecohydrologic characteristics under elevated CO_2 conditions observed using Free Air CO_2 Enrichment (FACE) technology.

[3] The multilayer canopy-soil-root system model incorporates both C3 and C4 photosynthetic pathways. Given that vegetation response to climate change is sometimes subtle, we hypothesize that accurately resolving the vertical light and thermal regimes within the canopy and representing the tight coupling between the leaf ecophysiology, energy balance and soil moisture state is required to predict the vegetation response to environmental perturbations. Bulk canopy, or "big-leaf," models do not resolve gradients in biological functioning or physical microenvironment through the canopy. This can result in errors in mass and energy exchange estimation [*Sinclair et al.*, 1976; *Norman*, 1979; *Pyles et al.*, 2000], and may be particularly problematic for understanding the impact of canopy structural changes, and biochemical and ecophysiological acclimation to climate variability.

[4] In this first part of the study, we present extensive validation of the model by examining its ability to accurately predict the whole canopy response typically observed using the eddy covariance technique, while at the same time resolving the vertical distributions of leaf states and fluxes within the canopy. We examine the role of the vertical distributions of leaf states in photosynthesis, and latent and sensible heat production. We also examine how these vertical distributions are impacted by soil moisture stress and how they manifest as canopy-scale observations typically made by flux towers. The study is performed for soybean (Glycine max; C3 photosynthetic pathway) and maize (Zea mays; C4 photosynthetic pathway) agricultural crops in the Midwestern United States. The companion paper [*Drewry et al.*, 2010] extends this analysis to an examination of observed plant acclimation under elevated CO_2 in the context of the SoyFACE (Free Air Carbon Enrichment) experimental facility in central Illinois [*Ort et al.*, 2006] where we examine the impact of elevated CO_2 on the vertically resolved leaf-level and canopy-integrated responses for both soybean and maize crops.

[5] Vertical variability in canopy processes is the result of a set of complex couplings between canopy structure [*Horn*, 1971; *Caldwell et al.*, 1986; *Ellsworth and Reich*, 1993], biochemical and ecophysiological properties of the vegetation [*Field*, 1983; *Amthor*, 1994; *Leuning et al.*, 1995], canopy environmental variation driven by turbulent mixing [*Raupach*, 1989; *Lai et al.*, 2000; *Albertson et al.*, 2001] and hydraulic gradients through the soil-root-plant system [*Williams et al.*, 1996; *Midgley*, 2003]. At the scale of a single leaf, or foliage layer, position within the canopy determines shortwave and longwave radiative forcing as a function of shading from surrounding foliage and proximity to plant and soil longwave sources [*Norman*, 1979]. The fluxes of carbon dioxide (F_c) and latent (LE) and sensible heat (H) from adjacent foliage layers and the soil determine environmental conditions which may differ significantly from those observed above the canopy [*Raupach*, 1989; *Baldocchi and Meyers*, 1998]. Absorbed photosynthetically active radiation excites photosynthesis, modulating stomatal conductance and thereby leaf temperature and the partitioning of available energy between transpiration and sensible heating. Stomatal conductance and leaf energy balance are controlled by the ambient environment of the leaf as well as the availability of soil moisture to supply moisture for transpiration [*Lhomme*, 1998; *Tuzet et al.*, 2003]. Accurate quantification of the impact of environmental change requires the consideration of the coupling between ecophysiology, biochemistry and the physical environment.

[6] A key determinant in the coupling between leaf biochemistry and stomatal conductance is the metabolic pathway exhibited by the vegetation. The CO_2 concentrating mechanism of C4 plants results in CO_2 saturated photosynthesis at ambient concentrations well below those currently experienced [*von Caemmerer and Furbank*, 1999]. In contrast to C3 vegetation, this effectively eliminates the sensitivity of carbon dioxide uptake to the direct impact of stomatal conductance through the control of the diffusion pathway between the ambient environment and the intercellular space [*Long et al.*, 2004; *Leakey et al.*, 2006b]. Indirect effects of stomatal closure, such as increases in leaf temperature and conservation of soil moisture, provide the most likely influences of stomatal conductance on C4 photosynthesis [*Long et al.*, 2004; *Ghannoum*, 2009]. The distinct modes of coupling between the ecophysiological processes of C3 and C4 vegetation necessitates their consideration in modeling efforts that attempt to disentangle the relative influences of environmental, structural and ecophysiological determinants of canopy behavior.

[7] The control of canopy functioning through its coupling to the soil environment by the root system can significantly impact the partitioning of energy and the magnitude of carbon uptake by vegetation [*Schulze and Hall*, 1982; *Tuzet et al.*, 2003; *Amenu and Kumar*, 2008]. Consideration of the soil column in bulk neglects the role of the vertical distribution of root biomass through the soil column and the advantages or limitations this places on moisture and nutrient acquisition [*Jackson et al.*, 2000; *Kleidon and Heimann*, 2000; *Feddes et al.*, 2001; *Schenk and Jackson*, 2002; *Siqueira et al.*, 2008; *Amenu and Kumar*, 2008]. A comprehensive mechanistic understanding and predictive capability of canopy-atmosphere exchange therefore requires vertically resolving the complexities inherent through the canopy-root-soil system.

[8] We utilize multiyear records of eddy covariance F_c, LE and H observations, collected at the Bondville (Illinois) AmeriFlux tower site, along with the meteorological variables required to drive the model, to examine model skill in capturing diurnal variation in fluxes over several growing seasons. This unique site offers the opportunity to examine

the influences of factors such as canopy structure and photosynthetic pathway on canopy-scale CO_2 uptake and energy exchange in a critical agro-ecosystem. Section 2 presents an overview of the model formulation (2.1), as well as details about the Bondville forcing and validation data (2.2) and the characterization of the canopy, soil and root system structures in the model (2.3). An analysis of the effects of varying canopy grid resolution are presented in section 3.1, followed by an evaluation of the model for soybean and maize using the half-hourly Bondville eddy-covariance data set in section 3.2. The role of meteorological conditions in controlling canopy-scale exchange of CO_2, latent and sensible heat are examined in section 3.3, providing an opportunity to further scrutinize model performance. Within-canopy variations of the radiation regime (section 3.4) and scalar fluxes (section 3.5) are inspected for the mean diurnal cycle over all study periods. This is followed by an analysis of the impact of water stress on canopy-scale and within-canopy scalar fluxes and water use efficiency in section 3.6. Focus is placed on the differences in canopy structure and photosynthetic metabolic pathways of soybean and maize as explanatory factors in their unique responses to water stress.

2. Materials and Methods

[9] Here we present features of the multilayer canopy-root-soil model (MLCan) which resolves the canopy radiation and meteorological microenvironment and leaf-level ecophysiological states at multiple canopy levels to determine canopy-atmosphere scalar fluxes (F_c, LE and H). The leaf-level processes are mediated by the photosynthetic metabolism exhibited by the vegetation, affecting stomatal conductance, leaf temperature and hence the partitioning of available energy between LE and H. MLCan was designed to allow flexibility in the choice of photosynthetic pathway, C3 or C4, while maintaining a consistent structure for the description of canopy-level and leaf-level processes that control land-atmosphere exchange, providing a framework for the evaluation of the role of photosynthetic metabolism on ecosystem processes. Following the brief presentation of the model, a description of data used for model forcing, validation and the specification of components of canopy and root system structure is given. Symbol definitions and units are presented in Table S1 in Text S1 (available as auxiliary material), as is the detailed formulation of MLCan.[1]

2.1. Model Formulation

[10] The model (see Figure 1) is driven by above-canopy observations of shortwave (R_g) and longwave (R_{lw}) incident radiation, air temperature (T_a), vapor pressure (e_a), ambient CO_2 concentration (C_a), wind speed (U) and precipitation (P). Consideration of photosynthetically active (PAR) and near-infrared (NIR) shortwave bands separately is required to account for the much higher absorptivity of PAR for green leaves [*Campbell and Norman*, 1998]. The model extends formulations such as CANOAK [*Baldocchi and Meyers*, 1998; *Baldocchi et al.*, 2002] and similar multilayer canopy models [e.g., *Gu et al.*, 1999; *Pyles et al.*, 2000; *Nikolov and Zeller*, 2003], with considerations for both C3 and C4 photosynthesis. As seen in Figure 2, at each canopy level photosynthesis is directly coupled to stomatal conductance and leaf energy balance. This allows us to examine the impact of not just differences in biochemical functioning of C3 and C4 plants, but also the effects of the coupling between biochemical, ecophysiological and physical functioning at the leaf-level, and how those interactions modify canopy-scale responses to environmental perturbations. While sophisticated hydrological considerations have been incorporated into a multilayer canopy model [*Williams et al.*, 1996], here we synthesize robust aboveground biophysical coupling and interactions with a root-soil hydrology model that explicitly represents the vertical variation in root conductivity. Our formulation includes a turbulent transport scheme that accounts for scalar gradients within the canopy space, and explicit representation of the gradients in water potential that drive moisture from the soil to root and supply moisture to the atmosphere by way of transpiration.

[11] Both PAR and NIR are attenuated through the canopy using a Beer's law approach [*Goudriaan*, 1977] that considers the leaf area at each canopy level and the clumping of foliage [*Campbell and Norman*, 1998]. The two shortwave bands are decomposed into direct and diffuse streams [*Spitters*, 1986], which allows for separate consideration of sunlit (f_{sun}) and shaded (f_{shade}) leaf fractions, as sunlit leaves receive both direct and diffuse radiation while the shaded fraction receives only diffuse radiation [*Spitters*, 1986]. These leaf fractions vary with depth in the canopy as a function of sun angle, canopy density and radiation intensity [*Spitters*, 1986; *Leuning et al.*, 1995]. The shaded canopy fraction is, by definition, only exposed to diffuse radiation, producing a set of leaf states (leaf temperature (T_l), stomatal conductance (g_s) and internal CO_2 concentration (C_i)) and fluxes generally differing from that of the sunlit fraction at each canopy level [*Leuning et al.*, 1995]. The canopy longwave regime is a function of both incident longwave from the atmosphere and the soil, and also that emitted by the foliage at each canopy level [*Baldocchi and Harley*, 1995]. The sunlit and shaded leaf fractions, which generally have different leaf temperatures, are thus distinguished when accounting for contributions to the longwave flux. The net gain in longwave energy (LW_{net}) at each canopy layer is the difference between the absorbed and emitted longwave flux magnitudes.

[12] Canopy-top observations of wind speed, air temperature and vapor pressure are applied as upper boundary conditions for the solution of the within-canopy microenvironment, with the canopy-top CO_2 concentration set to the mean ambient level experienced during the simulation periods (370 [ppm]). Wind is attenuated through the canopy as a function of leaf area density at each layer [*Poggi et al.*, 2004] allowing for calculation of boundary layer conductance for the "big leaf" at each level [*Nikolov et al.*, 1995]. A first-order closure is used to resolve within-canopy concentrations and air temperature as a function of the scalar flux distribution through the canopy [*Poggi et al.*, 2004; *Katul et al.*, 2004]. Water is captured by foliage surfaces both during precipitation events and through dew formation which has been shown to be significant at agricultural sites in the central United States [*Kabela et al.*, 2009]. Energy intercepted by wet surfaces is used for evaporation, requiring separate consideration of the energy balance of wet leaves [*Norman*, 1979; *Weiss et al.*, 1989]. Throughfall and soil surface evaporation

[1] Auxiliary materials are available in the HTML. doi:10.1029/2010JG001340.

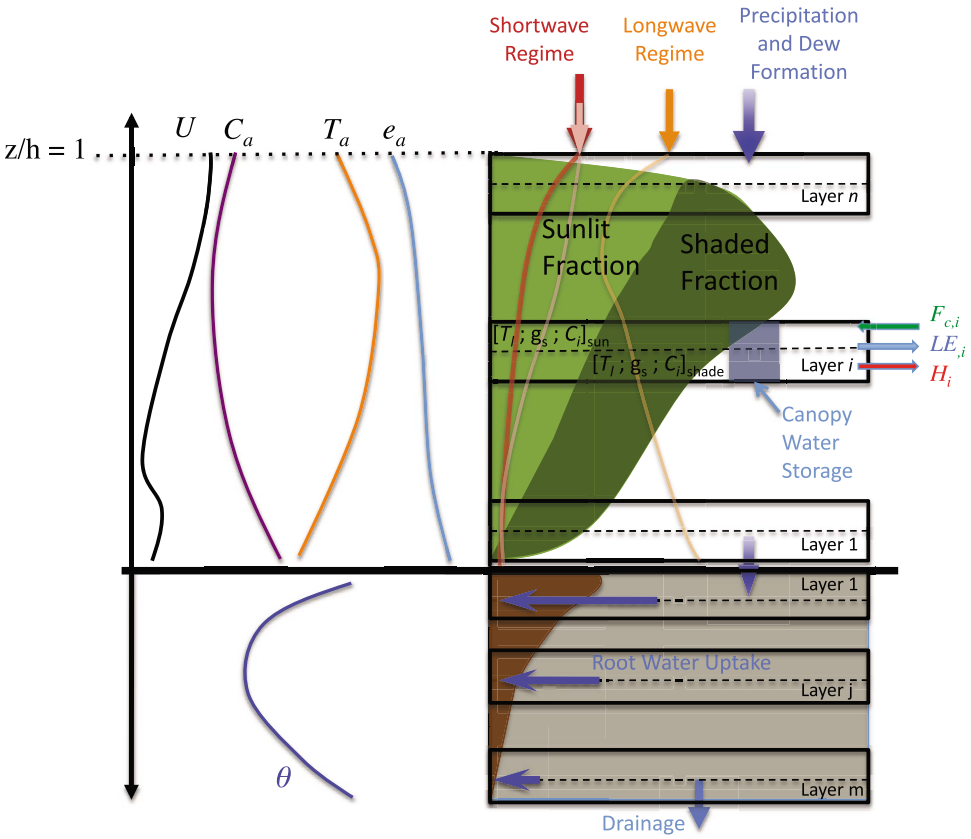

Figure 1. Schematic of the canopy, root, and soil system model. Shortwave radiation components (*PAR* and *NIR*) are attenuated through the canopy, accounting for absorbed, transmitted, and reflected fractions at each layer. Direct (red) and diffuse (pink) components of the shortwave streams are considered separately to account for sunlit and shaded leaf fractions at each canopy level. The longwave radiation regime accounts for absorption and emission by the foliage in each canopy layer. Incident radiation fluxes force the soil heat budget model. Wind speed is resolved within the canopy space, as are gradients in concentrations of CO_2, water vapor, and heat. Rainfall and dew accumulate on foliage, resulting in evaporation and a reduction in throughfall to the soil surface. Rainfall and dew replenish the subsurface moisture store that supplies the root system moisture for use in daytime evapotranspiration. A multilayer soil and root system model are used to compute moisture uptake through the root zone.

provide the surface flux boundary condition for the solution of soil moisture (θ).

[13] At the leaf-level, photosynthesis, energy balance, and stomatal and boundary layer conductances determine the flux densities of CO_2, water vapor, and heat as a function of ambient environmental conditions and radiative drivers (Figure 2). MLCan is capable of utilizing C3 or C4 metabolism, allowing for the role of biochemical responses to environmental variability to be considered within the same general leaf- and canopy-level framework.

[14] The dashed arrow in Figure 2 connecting stomatal conductance and photosynthesis signifies that this connection may not generally be important for the determination of A_n in C4 plants, due to the CO_2 concentrating mechanism of C4 physiology that effectively decouples A_n from g_s across a wide range of conditions typically experienced [*Hatch*, 1987; *Furbank et al.*, 1989; *Collatz et al.*, 1992]. Net leaf fluxes at each canopy level are calculated as a weighted average of the sunlit and shaded leaf fluxes and those from the wet leaf fraction. Photosynthetic capacity, as represented by the maximum rates of ribulose-1,5-bisphosphate (RuBP) regeneration and RuBP carboxylase-oxygenase (Rubisco) catalyzed carboxylation at 25°C ($J_{max,25}$ and $V_{cmax,25}$, respectively), declines exponentially through the canopy, affecting A_n and leaf respiration at each canopy level. Canopy-scale fluxes are computed through the vertical integration over each of the foliage layers.

[15] Leaf respiration is calculated as a function of foliage photosynthetic capacity, which varies vertically through the canopy accounting for broadly observed reductions in leaf nitrogen content from the canopy top. The other components of the ecosystem respiration (ER) flux are generally difficult to observe, requiring continuous respiration samples for various plant and soil components [e.g., *Lavigne et al.*, 1997; *Wilson and Meyers*, 2001; *Palmroth et al.*, 2005]. Nocturnal eddy covariance observations under well mixed conditions provide estimates of ER. Despite differences in crop residue for the soybean and maize crops examined here [*Hollinger et al.*, 2005], the functional relationship between nocturnal eddy covariance CO_2 fluxes and air temperature were very

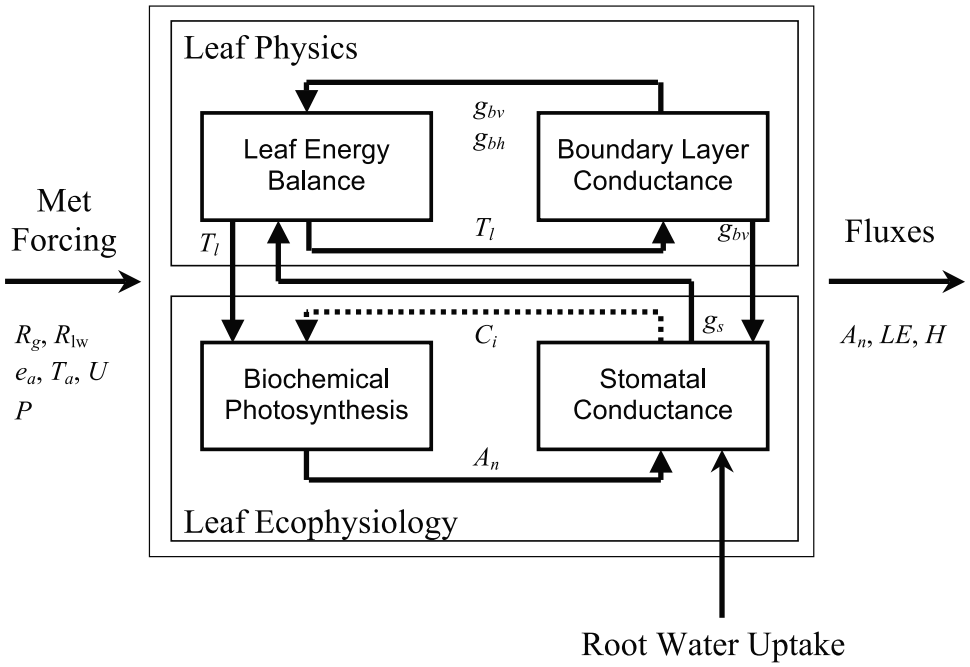

Figure 2. Leaf-level model component coupling. Observed meteorological conditions drive the leaf-level ecophysiological (photosynthesis and stomatal conductance) and physical (boundary layer conductance and energy balance) component models. The components are coupled by the boundary layer conductances to vapor and heat (g_{bv} and g_{bh}), leaf temperature (T_l), net CO_2 uptake (A_n), internal CO_2 concentration (C_i), and stomatal conductance (g_s). Reduced root water uptake under periods of stress can constrain stomatal conductance. Outputs include the flux densities of CO_2, latent and sensible heat for the canopy layer.

similar, with the mean ER values for each crop falling within the standard deviation of that of the other crop across a range of temperature classes from 10 to 30°C. Due to these factors we use here a simple formulation that accounts for the widely observed temperature dependence of ER. Net ecosystem CO_2 exchange is then calculated as the difference between the net canopy uptake and ER.

[16] Moisture uptake from the soil by the root system provides water for transpiration, with soil water deficits acting to constrain leaf-level fluxes through a control on leaf water potential (Ψ_l) that results in decreased stomatal conductance and plant gas exchange [*Jones*, 1973, 1992; *Lhomme*, 1998; *Tuzet et al.*, 2003; *Bunce*, 2004]. Root system structure, in particular the distribution of conductive elements through the soil column, acts in concert with the vertical distribution of soil moisture to determine the availability of moisture to the plant [*Schenk and Jackson*, 2002; *Amenu and Kumar*, 2008]. MLCan utilizes a vertically resolved soil column [*Oleson et al.*, 2004], with root conductivity distributed according to observed profiles of root biomass [*Tufekcioglu et al.*, 1998; *Schenk and Jackson*, 2002]. Radial root conductivities determine the ability of the root system to absorb moisture from the soil [*Amenu and Kumar*, 2008]. The root distribution-weighted pressure potential ($\Psi_{r,wgt}$) and the transpiration requirement of each canopy layer determine the distribution of Ψ_l through the canopy [*Brisson et al.*, 1993]. Plant hydraulic conductance is reduced as Ψ_r becomes more negative [*Blizzard and Boyer*, 1980], further regulating Ψ_l potentially to guard against xylem cavitation [*Tyree and Sperry*, 1988; *Sperry*, 2000]. Parameter values representing the radiative, biochemical, stomatal and subsurface characteristics of the soybean and maize canopies are listed in Table 1.

2.2. Model Forcing and Validation Data

[17] This study utilizes an extensive data set collected at the Ameriflux tower site located in Bondville, Illinois (40.0062 Latitute, −88.2904 Longitude, 219 m above sea level). Continuous measurements of a range of meteorological and flux variables were obtained from an instrumented 10 m tower located in a field that has undergone an annual rotation between soybean (even years) and maize (odd years) since observations began in 1996. Net radiation (R_n), downward shortwave and longwave energy fluxes were measured with a net radiometer and quantum sensor at the top of the tower. For periods when R_{lw} observations were not available or were of poor quality, the algorithm of *Brutsaert* [1982] was used. The separation of *PAR* and *NIR* fractions is performed by applying the standard assumption that approximately half of R_g is *PAR* and the other half is *NIR* [*Campbell and Norman*, 1998]. The diffuse fraction of R_g is determined as a function of solar zenith angle and day of year using an estimate of the theoretical extraterrestrial shortwave flux that would be incident in the absence of vapor and other gases that interact with shortwave in the atmosphere [*Spitters*, 1986]. Zenith angle is computed as a function of site location, day of year and time of day according to the algorithm presented by *Campbell and Norman* [1998].

[18] A tipping bucket rain gauge produced estimates of precipitation. Meteorological conditions, including wind speed, air temperature and humidity were observed from instrumentation on the tower. Eddy covariance CO_2 and

Table 1. Parameter Listing for the Soybean and Maize Application Using MLCan

Description	Symbol	Units	Soybean	Maize
C3 Photosynthesis[a]				
Fraction absorbed Q available to photosystem II	β_f	-	0.5	
Maximum rate of Rubisco-limited carboxylation at 25°C	$V_{c\max,25}$	μmol m^{-2}s	100	
Maximum electron transport rate at 25°C	$J_{\max,25}$	μmol m^{-2} s	180	
C4 Photosynthesis[b]				
Intrinsic quantum yield of C3 photosynthesis	α_r	mol mol^{-1}		0.035
Initial slope of C4 photosynthetic CO_2 response	k_4	mol m^{-2} s^{-1}		0.7
Reference value for leaf respiration	$R_{d,4}$	μmol m^{-2} s^{-1}		0.8
Reference value for substrate saturated Rubisco capacity	$V_{\max,4}$	μmol m^{-2} s^{-1}		40
Temperature sensitivity of temperature-dependent C4 parameters	$Q_{10,4}$	-		2.0
Conductance and Leaf States[c]				
Ball-Berry slope	m	-	10.6	7
Ball-Berry intercept	b	mol m^{-2} s^{-1}	0.008	0.008
Stomatal sensitivity parameter	s_f	MPa^{-1}	3.5	6.5
Ψ_l at which half potential g_s is lost	Ψ_f	MPa	−1.3	−1.3
Leaf forced convection parameter	c_f	-	$4.3\cdot10^{-3}$	$4.3\cdot10^{-3}$
Leaf free convection parameter	c_e	-	$1.6\cdot10^{-3}$	$1.6\cdot10^{-3}$
Canopy Structural[d]				
Canopy height	h	m	1	2.5
Displacement height	d	m	2/3h	2/3h
Leaf width	d_o	m	0.06	0.08
Foliage clumping factor	Ω	-	0.8	1.0
Maximum H_2O storage capacity of a leaf	S_m	mm $(LAI)^{-1}$	0.2	0.2
Foliage drag coefficient	C_d	-	0.2	0.2
Mixing length coefficient	α	-	0.13	0.13
Decay coefficient for leaf nitrogen content	k_n	-	0.5	0.5
Radiation and Energy Balance[e]				
Leaf emissivity	ϵ	-	0.96	0.94
Atmospheric emissivity	ϵ_a	-	0.80	0.80
Soil surface emissivity	ϵ_s	-	0.90	0.90
Leaf absorptivity to *PAR*	α_p	-	0.80	0.80
Leaf absorptivity to *NIR*	α_n	-	0.15	0.23
Diffuse extinction coefficient	K_d	-	0.55	0.6
Leaf angle distribution parameter	x	-	0.81	1.64
Soil Flux and State Parameters[f,g]				
Fractional soil sand content	f_s	-	0.05	0.05
Fractional soil clay content	f_c	-	0.25	0.25
Soil respiration rate at 10°C	R_o	μmol m^{-2} s^{-1}	1.2	1.2
Temperature sensitivity of soil respiration rate	Q_{10}	-	2	2
Soil surface roughness length	z_o	m	0.005	0.005
Root System Properties[h]				
Root depth	r_d	m	1.5	1.5
50th percentile rooting depth	z_{50}	m	0.28	0.28
95th percentile rooting depth	z_{95}	m	0.92	0.92
Radial conductivity per unit fine root area	$K_{r,unit}$	s^{-1}	$1.52\cdot10^{-9}$	$1.52\cdot10^{-9}$
Total root system radial conductivity	$K_{r,tot}$	s^{-1}	$1.2\cdot10^{-7}$	$1.2\cdot10^{-7}$
Total fine root area	R_{fr}	m^2 m^{-2}	79.1	79.1

[a] *Bernacchi et al.* [2003, 2005a].
[b] *Collatz et al.* [1992].
[c] *Leakey et al.* [2006a], *Bunce* [2004], and *Nikolov et al.* [1995].
[d] *Campbell and Norman* [1998], *Katul et al.* [2004], *Anderson et al.* [2000], *Nikolov and Zeller* [2003], *Kabela et al.* [2009], and *Meyers et al.* [2010].
[e] *Campbell and Norman* [1998].
[f] *Hinzman et al.* [1998] and *Meyers et al.* [2010].
[g] Respiration parameters deduced from nocturnal eddy covariance observations.
[h] *Tufekcioglu et al.* [1998], *Anderson et al.* [2000], *Huang and Nobel* [1994], and *Jackson et al.* [1997].

energy flux estimates between the canopy and overlying atmosphere were made with a sonic anemometer mounted in close proximity to an open path gas analyzer, each operating at high frequency. We refer to previously published site descriptions [*Meyers and Hollinger*, 2004; *Bernacchi et al.*, 2005b; *Hollinger et al.*, 2005] for further details concerning the instrumentation, measurement and averaging protocols, and site characteristics. In this study, half-hourly averages of all forcing data and fluxes are used for simulation and validation purposes. Ameriflux (http://public.ornl.gov/ameriflux/) L4 gap-filled forcing data was used to provide a continuous record of the required forcing variables when data quality or sensor failure produced gaps in the observational records.

Table 2. Mean Environmental Variables and Total Precipitation Observed for Each Simulation Period Over the 6 Study Years

Cover	Year	Simulation DOYs	$\overline{R}_g$ (W m^{-2})	$\overline{T}_a$ (°C)	$\overline{D}$ (kPa)	$\overline{U}$ (m s^{-1})	$\overline{P}_{day}$ (mm)
Maize	2001	184–232	643.5	25.5	1.0	3.1	1.9
	2003	214–237[a]	606.6	24.9	0.9	2.7	1.2
	2005	189–244	529.0	25.8	0.9	2.4	2.9
Soybean	2002	213–258	545.4	24.8	0.9	3.4	0.9
	2004	185–241	594.5	22.6	0.6	3.4	4.3
	2006	189–241	524.3	25.4	0.7	2.7	7.8

[a]Number of days reduced from the period for which $LAI \geq 3.5$ due to crop damage from ice storm [*Bernacchi et al.*, 2007].

[19] The simulation period for each year spans the days in which leaf area index (*LAI*) was greater than 3.5 [m^2 m^{-2}] (see Table 2 and Figure 3), except for 2003 during which an ice storm caused significant damage, resulting in canopy closure at day 214 [*Bernacchi et al.*, 2007]. The 2002 growing season was the driest period examined in this study, with an extended interval of negative Palmer Crop Moisture Index (PCMI) values indicating moderate drought stress (PCMI ≤ -1) [*Leakey et al.*, 2006b]. The 2001 growing season was the driest study period for the maize canopy, which was characterized by periods of negative PCMI as well. The 2003 and 2005 study periods also have periods without significant rain that span 1–2 weeks in duration, with half of the rainfall occurring in the later parts of the study period for both of these years.

2.3. Canopy, Soil, and Root System Structure

[20] The model requires specification of the structural characteristics of the canopy, root and soil systems. Canopy structure is described by a leaf area density (*LAD* [m^2 m^{-3}]) profile. For the soybean canopy, *LAD* profiles observed in August of 2002 [*Dermody et al.*, 2006] were averaged and normalized by dividing by the canopy leaf area index at the time of measurement (Figure 4a). The normalized *LAD* profile was then used at each model time step to distribute observed *LAI* vertically through the canopy. A similar procedure was used for maize, in which a function fit to a set of maize *LAD* profile observations [*Boedhram et al.*, 2001] was used (Figure 4a). The maize profile is generally smoother and more uniform than the soybean profile, with a maximum at $z/h \simeq 0.6$. The soybean profile is characterized by a large peak at $z/h \simeq 0.85$, with the top third of the canopy containing 46% of the leaf area. The model currently does not consider leaf morphology.

[21] The distribution of roots through the soil column is performed using the logistic dose-response curve used by *Schenk and Jackson* [2002] (Figure 4b), with 50% and 95% cumulative root distribution function parameters (see Table 1) set to values that concentrate root biomass in the upper 50 cm of the soil column, with maximum rooting depths of 1.5m for both maize and soybean [*Tufekcioglu et al.*, 1998]. Soil composition is set uniformly to 25% clay, 5% sand and 70% silt, with a bulk density of 1.5 [g cm^{-3}], as specified on the Ameriflux Bondville site data page, given no information about vertical variation of these quantities with depth. The model is initialized with θ profiles set equal to 0.3 [m^3 m^{-3}], or 90% of field capacity as determined by a 21 day dry-down simulation with no vegetation influence, for all study years except 2002. The drought in 2002 [*Leakey et al.*, 2006b] motivated the initialization of the moisture profile to 70% of field capacity, or 0.23 [m^3 m^{-3}]. Observations of the fractional reduction in g_s with decreases in Ψ_l were extracted digitally from *Bunce* [2004] and fit to the sensitivity function presented by *Tuzet et al.* [2003] (Figure 4c).

[22] Leaf-area index was measured at biweekly intervals during the growing seasons and interpolated to daily resolution (Figure 5). Data was collected using a plant canopy analyzer (LAI-2000, Li-Cor, Lincoln, NE, United States) which estimates *LAI* based on the probability that light would not contact vegetation as it passed through the canopy [*Lang*, 1991; *Welles and Norman*, 1991]. Measurements were made within 2 h of sunrise when incident light was diffuse. *LAI* measurements were made at three locations throughout the field. Each sampling consisted of three subsamples, with each subsample consisting of one measurement above and five measurements below the canopy. Thus, each replicate *LAI* measurement included 3 above-canopy and 15 below-canopy readings. A view cap, which excluded 50% of the field of view, was used to exclude the instrument operator.

3. Results and Discussion

[23] The effects of vertical layering on the resolution of the canopy environment and canopy-atmosphere scalar exchange for the two agricultural species are first examined below. Having identified a sufficient number of canopy layers we apply the model to 7488 half-hour simulation periods for the soybean canopy over the 2002, 2004 and 2006 growing seasons, and 6192 half-hour simulation periods for the maize system over the 2001, 2003, 2005 growing seasons. Model performance is examined in terms of the correlation between modeled and observed fluxes and diurnal flux trends. An analysis of the impact of meteorological conditions provides a basis for further examining the fidelity of the model to observations, as well as providing insight into the controls of R_g, T_a, *VPD* and U on canopy-atmosphere exchange for maize and soybean. The vertical resolving power of the model is applied to absorbed shortwave and net longwave radiation through the canopy space of both crops, with a focus on the relative roles of sunlit and shaded leaf fractions through an average diurnal cycle. This is followed by an examination of the diurnally averaged exchange rates of CO_2, water vapor, sensible heat and net radiation, for which the radiation regime previously described is the primary forcing. The roles of vertical canopy structure and canopy density are examined in the context of the resolved radiation regime and flux profiles. The effects of soil moisture deficit on aboveground canopy functioning are finally presented. Within-canopy and vertically integrated flux responses of increasing moisture deficit, quantified by the canopy-average reduction in g_s through the hydraulic constraint depicted in Figure 4c are examined

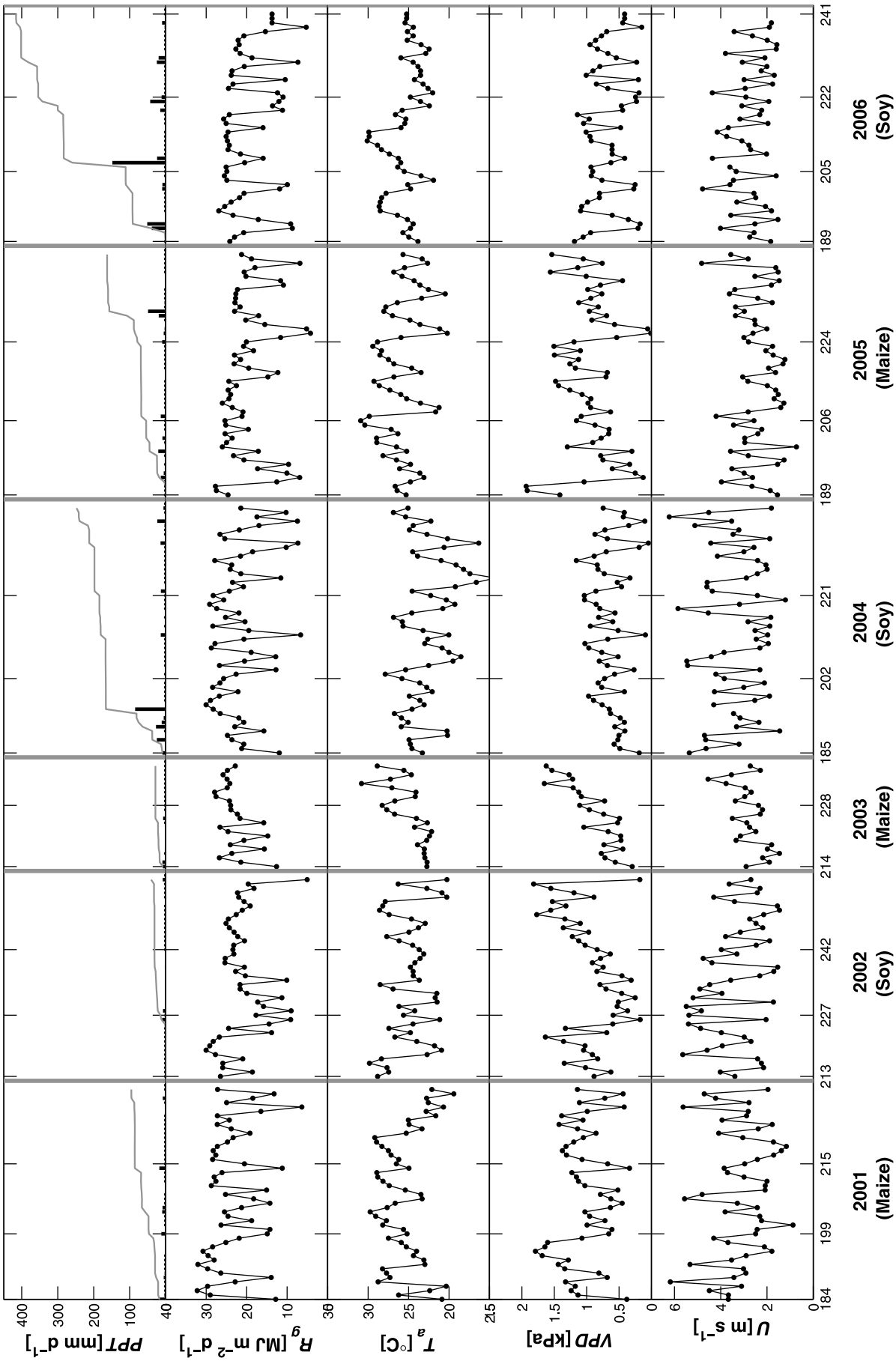

Figure 3. Total daily (black lines) precipitation (P) and daily total downwelling shortwave (R_g); mean daytime air temperature (T_a), vapor pressure deficit (VPD), and wind speed (U); and cumulative P (gray lines) for the growing season study periods in 2001–2006.

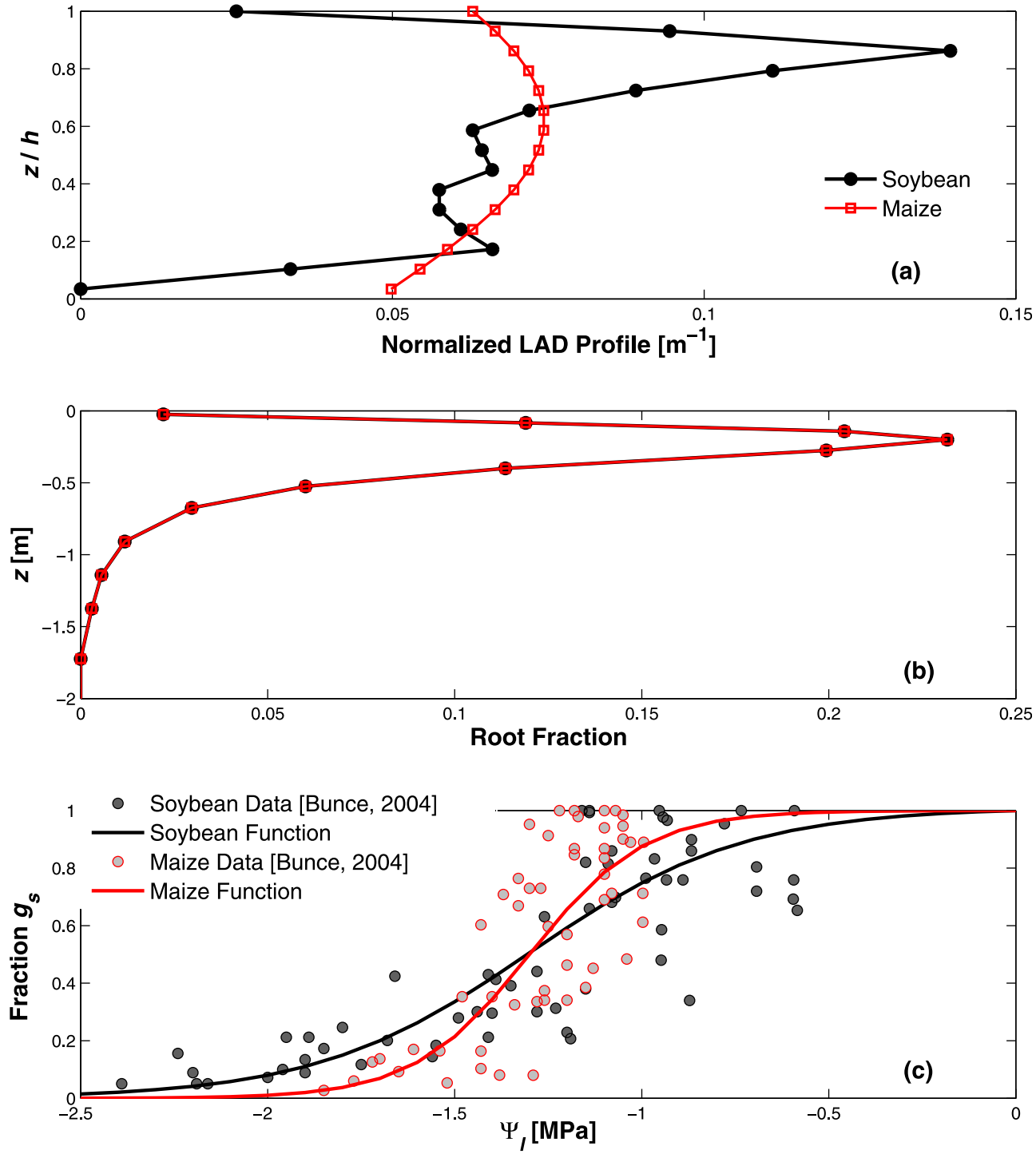

Figure 4. (a) Canopy *LAD* profiles for soybean (black dots) and maize (red squares), (b) root fraction in each soil layer, and (c) the functional dependencies of the stomatal conductance on leaf water potential (Ψ_l). Data from *Bunce* [2004] used to fit the functional dependencies in Figure 4c are also presented. The vertical axis in Figure 4a is normalized by the height of the canopy (1 m for soy, 2.5 m for maize) to facilitate comparison between the two canopy structures.

through differences in canopy structure and photosynthetic metabolism of the two crops. Throughout this section, daytime conditions refer to those periods for which $R_g >$ 10 [W m^{-2}], and nocturnal periods correspond to all other data points.

3.1. Effects of Vertical Resolution

[24] A set of model runs was conducted to examine the effect of vertical canopy resolution (number of layers used to subdivide the canopy) on model estimates of leaf states and

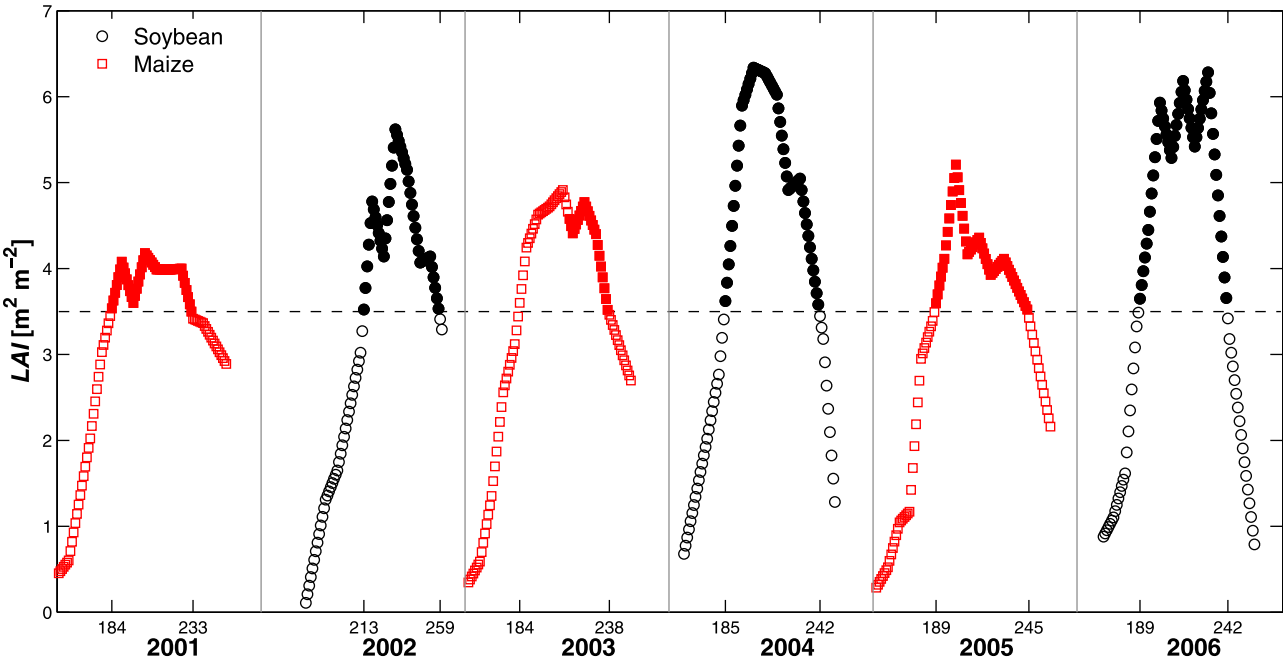

Figure 5. Daily variation of leaf area index for the soybean (black circles) and maize (red squares) canopies as observed at the Bondville Ameriflux site over the 2001–2006 growing seasons. A dashed line denotes $LAI = 3.5$ (m^2 m^{-2}) which was used to determine the simulation periods for each growing season (solid symbols). Simulations began on DOY 214 in 2003 due to canopy damage caused by an ice storm [*Bernacchi et al.*, 2007].

fluxes and to determine a suitable number of layers for this study and the companion paper [*Drewry et al.*, 2010]. *Norman* [1979] suggests as a general rule that a maximum leaf area of 0.5 [m^2 m^{-2}] be used for each model layer to accurately apply statistical canopy radiative transfer models. Factors such as the shape of the leaf area profile [*Wu et al.*, 2000] and the inclination angles of leaves through the canopy [*Baldocchi et al.*, 2002] can likewise have an impact on the required number of layers to accurately simulate the canopy radiation regime and consequently canopy-atmosphere mass and energy exchange [*Pyles et al.*, 2000]. The model was run with [2, 3, 4, 5, 6, 7, 8, 9, 10, 15, 20, 25, 30, 35, 40, 45, 50] canopy layers, and the changes in several canopy states and fluxes were examined as the vertical resolution of the canopy was varied. Figure 6a presents the diurnally averaged sunlit leaf fraction of the entire maize canopy for a subset of these simulations. The total sunlit fraction at noon increases from approximately 28% to 40% as the canopy resolution increases from 3 to 50 layers. In Figure 6b, the cumulative fraction of incident *PAR* absorbed through the depth of the maize canopy is plotted. Agreement between the low- and high-resolution canopies seen at the canopy top declines with depth, as the more finely resolved canopies allow for better accounting of reflected radiation and its absorption by neighboring layers.

[25] Figure 6c presents the vertical distribution of mean leaf temperature, and Figure 6d presents the vertical distribution of the sunlit and shaded canopy fractions for the maize canopy at 1200 local time. The mean leaf temperature is calculated as the average between the temperatures of the sunlit and shaded leaf fractions, weighted by the fraction of sunlit and shaded leaves in each layer. The mean canopy temperature between the lowest and highest resolution canopies differs by several tenths of a degree relatively uniformly through the canopy. The sunlit leaf temperature of the three-layer canopy is greater than that of the higher-resolution canopies, but the lower temperature of the shaded fraction, in combination with the larger fraction of leaf area being allocated to shaded leaves in the low resolution canopy, results in lower mean canopy temperatures. The mean, sunlit, and shaded g_s are presented in Figures 6e and 6f. The upper-canopy g_s is lower for the low-resolution canopies, resulting from the slightly lower shaded g_s and the greater shaded canopy fraction, relative to the more highly resolved canopies.

[26] Figure 6g presents the difference in total *PAR* absorbed by each canopy relative to that absorbed by the 50-layer canopy. As the canopy becomes more finely resolved, greater leaf area is sunlit (Figure 6a) and thus the total absorbed by the shaded fraction declines, while that absorbed by the sunlit fraction increases. The net result is an approximately 20% increase in total *PAR* absorption with a 50-layer canopy relative to a three-layer canopy. The difference for sunlit and shaded absorption is within 5% once the canopy has been discretized into 15 layers. The impact of layering on total canopy fluxes of CO_2, latent and sensible heat are presented in Figure 6h, where the effect of greater *PAR* (Figure 6g) and *NIR* (results not shown) absorption can be seen for all three fluxes. Each flux for both soybean and maize increases with

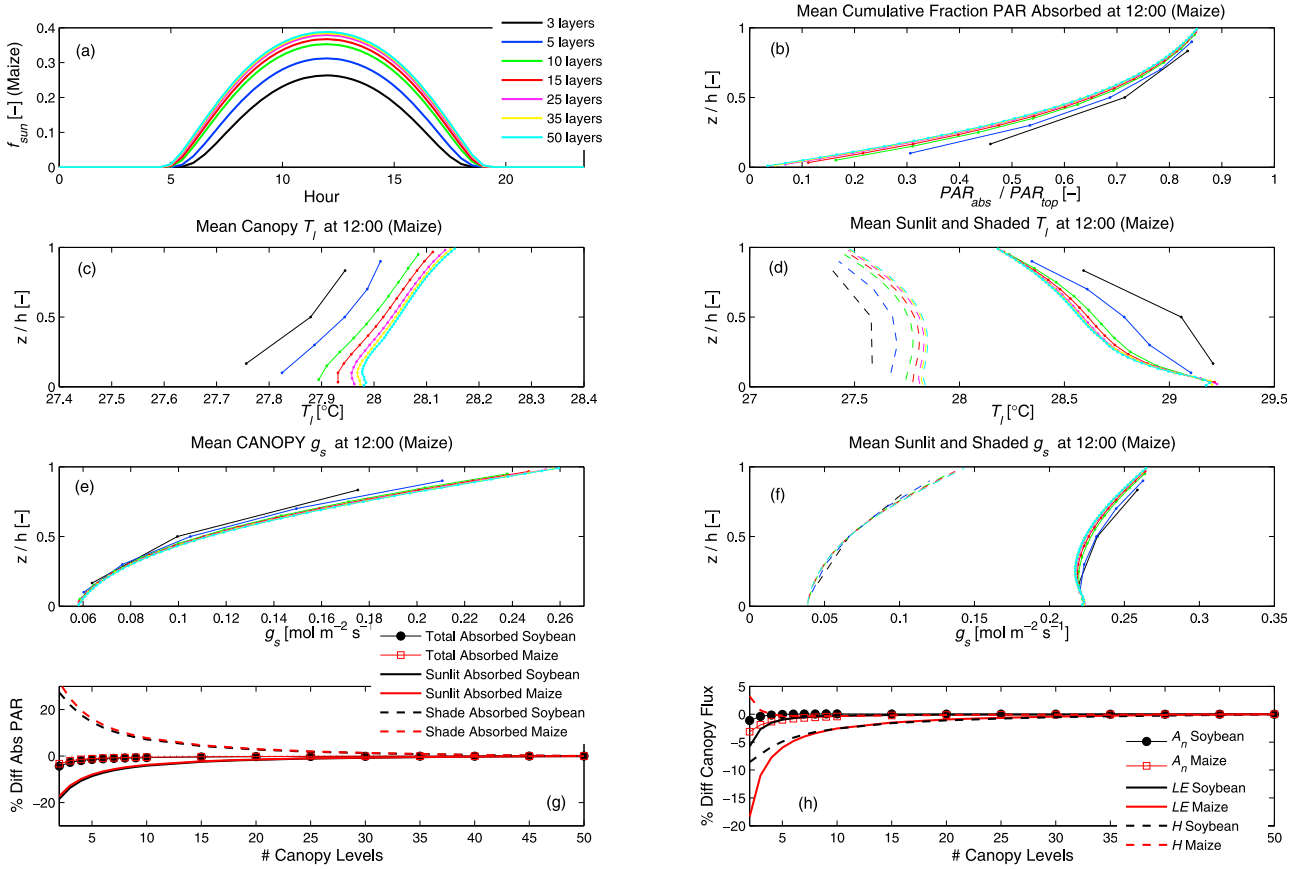

Figure 6. Sensitivity analysis of the effect of vertical canopy resolution on (a and b) canopy radiation regime, (c-f) leaf states, and (g and h) net canopy-atmosphere fluxes. In Figures 6d and 6f, shaded foliage profiles are presented as dashed lines, and sunlit foliage profiles are presented as solid lines with dots.

additional layering, with the exception of H for maize. For these two canopies, LE is generally at least three times greater than H in the middle of the day (results presented below), meaning that for both soybean and maize, an increase in canopy layering results in greater total available energy ($LE + H$) due to the greater fraction of shortwave absorbed. The difference in A_n is relatively small, with less than 5% change from 3 to 50 layers.

[27] For the soybean and maize canopies examined here, a 15-layer discretization differs by only a few percent relative to the 50-layer canopy with respect to midday sunlit canopy fraction, sunlit and shaded PAR absorption, and net canopy-atmosphere CO_2 and energy exchange. This is in general agreement with *Pyles et al.* [2000], who found that 20 canopy layers was generally sufficient to accurately model surface fluxes, with a 10-layer discretization introducing significant errors. For the peak LAI of approximately 6.5 [m^2 m^{-2}] examined in this study (see Figure 5), the average LAI per layer is 0.43. We conclude from the negligible improvement in net canopy radiation absorption and fluxes for resolutions beyond 15 layers that a 15-layer discretization is sufficient for the soybean and maize canopies examined in this study.

3.2. Model Validations: Half-Hourly Simulation Performance

[28] Overall, the model demonstrated significant skill in capturing the mean diurnal variations in canopy-atmosphere exchange over the three growing seasons (Figures 7 and 8). The one-to-one plots show reasonable agreement between the half-hourly modeled and observed fluxes, with the slopes of the lines fit to the modeled and observed fluxes differing by no more than 16%. The apparent plateau in daytime net CO_2 exchange is the result of using fixed seasonal average values of canopy-top photosynthetic capacity over the simulation periods. Photosynthetic parameters ($V_{cmax,25}$ and $J_{max,25}$) as well as parameters describing the relationship between photosynthesis and stomatal conductance have been shown to vary seasonally [*Wilson et al.*, 2000a; *Xu and Baldocchi*, 2003] and interannually [*Ellsworth*, 2000]. This temporal variability in vegetation functioning has been linked to leaf aging [*Wilson et al.*, 2000b] which may produce a more pronounced effect for annual crops whose life spans extend across a single season. There also is evidence for temporal variability in parameters that describe components of eco-

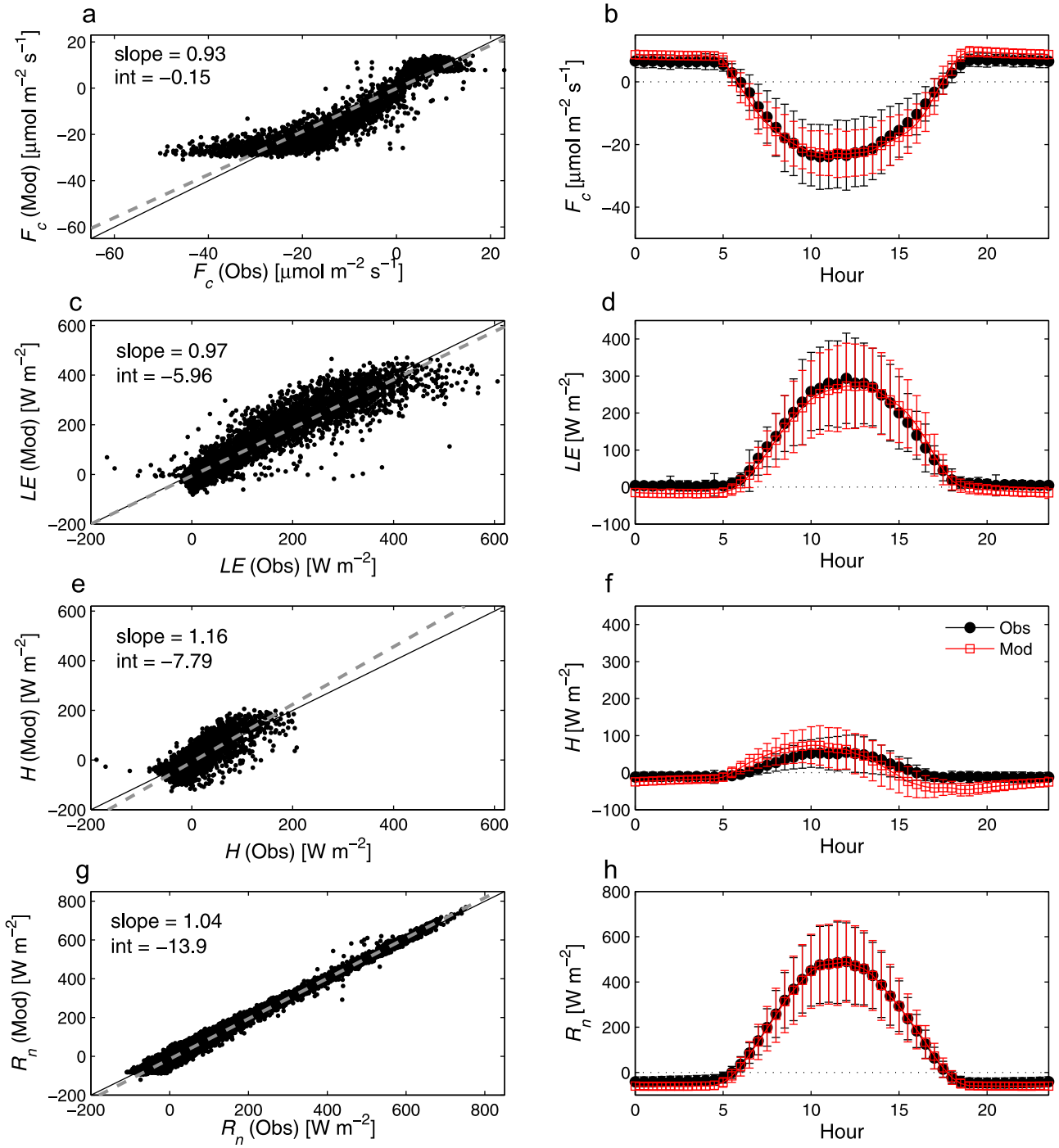

Figure 7. Model-data comparison of net canopy-atmosphere fluxes of (a and b) CO_2 flux, (c and d) latent heat, (e and f) sensible heat flux, and (g and h) net radiation for 7488 half-hour soybean study periods. (left) Comparison of modeled (vertical axis) and observed (horizontal axis) fluxes. The 1-1 line is presented as a diagonal black line. The linear regression between modeled and observed fluxes is presented as a dashed gray line, with the slope and intercept listed. (right) The diurnally averaged fluxes obtained from the model (red squares) and observations (black dots), with vertical bars representing ± one standard deviation. RMSE of half-hourly F_c, LE, H, and R_n for soybean were 3.3 (μmol m^{-2} s^{-1}), 33.3 (W m^{-2}), 27.3 (W m^{-2}), and 23.0 (W m^{-2}), respectively.

system respiration [*Janssens and Pilegaard*, 2003], which may be due to factors such as ecosystem substrate supply [*Davidson et al.*, 2006]. For this study, however, we focus on the temporal average behavior of each canopy, and seek to address these important issues related to seasonal and interannual variability in CO_2 exchange in future work.

[29] The model appears to underpredict nocturnal LE, with simulated values slightly negative, whereas the eddy

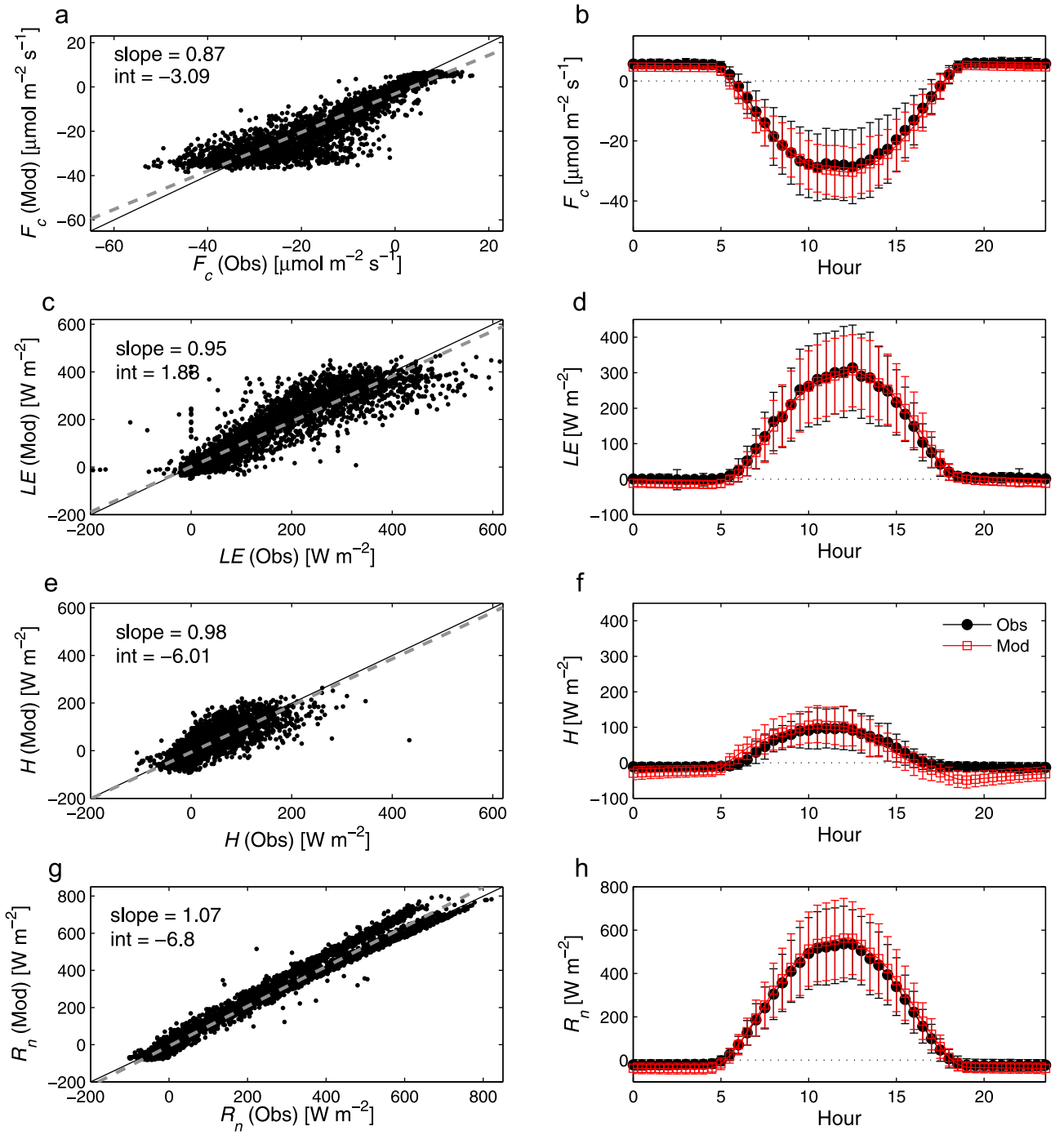

Figure 8. Model-data comparison of net canopy-atmosphere fluxes for 6192 half-hour maize study periods. All information is as presented for soybean in Figure 7. RMSE of half-hourly F_c, LE, H, and R_n for maize were 3.0 (μmol m^{-2} s^{-1}), 34.0 (W m^{-2}), 33.0 (W m^{-2}), and 33.3 (W m^{-2}), respectively.

covariance estimates indicate no nocturnal latent energy flux. These calculated negative *LE* values are the result of dew formation, which has been observed to frequently occur for agricultural crops in this region [*Kabela et al.*, 2009]. A reasonable explanation for the discrepancy is the well known unreliability of the eddy covariance technique when the atmosphere is stably stratified [*Massman and Lee*, 2002; *Goulden et al.*, 1996; *Moncrieff et al.*, 1996], as is often the case at night when the surface cools faster than the overlying air, resulting in a strong near-surface temperature inversion. Minor discrepancies in energy flux partitioning are also apparent in the late afternoon, when *LE* is slightly overpredicted and *H* correspondingly underpredicted. The net radiation at the canopy top is in close agreement with observations, indicating that the modeled radiation regime is properly accounting for incident shortwave and longwave radiation.

[30] MLCan produced a similar level of agreement in estimated canopy-top fluxes for the C4 maize canopy (Figure 8) as was the case for the C3 soybean canopy discussed above. Slopes of the one-to-one comparisons are again reasonable, with very good agreement in mean diurnal flux magnitudes. Dew deposition again produced negative *LE* for the diurnal means spanning nocturnal periods. The estimates of net radiation at the canopy top are also in excellent agreement with observations, indicating that the radiation regime is adequately simulated for the less dense maize canopy, with a mean *LAI* over the study periods of 4.1 [m^2 m^{-2}], relative to 5.1 for soybean (see Figure 5). Total differences in diurnally averaged F_c, *LE*, *H* and R_n over the course of a day, as a percentage of the total observed flux were (3.9%, −3.1%, 0.5% and −1.0%) and (8.0%, −0.7%, 2.8% and 6.0%) for soybean and maize, respectively.

[31] We also examined the impact that the exponential decrease in photosynthetic capacity from the top of the canopy (see equation (7) in Text S1) has on CO_2 uptake and energy partitioning. An additional simulation was run for each canopy, in which the photosynthetic capacity through the canopy was specified uniformly to be that of the top leaf. Over the 3 year study period for each canopy, the mean diurnal increase in A_n was 49.8% for the soybean canopy and 16.8% for the maize canopy. The uniform profiles also resulted in an reduction in leaf temperature through the canopies due to an increase in *LE* of 14.5% and 5.2% for soybean and maize, respectively. The greatest gains in CO_2 uptake are made for sunlit leaves in the upper region of the canopies, where the increase in photosynthetic capacity significantly increases the magnitude of photosynthesis for light-saturated foliage.

[32] Figure 9 demonstrates the sensitivity of variations in canopy-top photosynthetic capacity, and vertical variation in the distribution of photosynthetic capacity, on simulated F_c. As seen in Figures 9a and 9b, modification of the photosynthetic capacity of the canopy-top leaves, which causes an increase in photosynthetic capacity through the canopy by way of equation (7) in Text S1, causes some increase in CO_2 uptake, with a greater effect for maize. Making the vertical distribution of photosynthetic capacity through the canopy uniform further increases CO_2 uptake, with a more dramatic effect for soybean. The effect of a uniform photosynthetic capacity distribution is seen in the 6 day traces of F_c, along with default and uniform photosynthetic capacity distribution simulations, presented in Figures 9c and 9d. The uniform photosynthetic capacity distribution simulation produces overestimates for both canopies on these days, with the maize simulation in closer agreement with observations. We note that disagreement between modeled and observed F_c could be the result of misspecification of several parameter values, in particular those describing ecosystem respiration sensitivity to temperature. These results provide some evidence that temporal variations in photosynthetic capacity and its distribution need to be observed periodically to better constrain model performance.

[33] Model performance under open-canopy conditions was examined by running the model for each crop cover for periods in which *LAI* was less than 3.5 [m^2 m^{-2}] (results not shown). For both canopies, under open canopy conditions net CO_2 uptake was overestimated, with maize showing mean errors of up to 8 [μmol m^{-2} s^{-1}] at noon, and errors of approximately 4 [μmol m^{-2} s^{-1}] for soybean at noon. The differences between the magnitudes of the errors produced by the two crops may be due to canopy closure at lower *LAI* values for the soybean canopy. Simulated CO_2 exchange is sensitive to specification of photosynthetic, respiration and other biophysical parameters and their variation through the canopy. We hypothesize that seasonal variability in leaf-level photosynthetic capacity and its vertical variation through the canopy plays a significant role in these errors, but more information on this variability is needed to address this issue.

[34] For open canopy conditions, *LE* and R_n were both estimated reasonably well by the model with respect to half-hourly one-to-one and mean diurnal comparisons. The sensible heat fluxes for both canopies were significantly underestimated for both crops, however. As *Bernacchi et al.* [2007] point out, periods when the canopy is open are disproportionately influenced by the dark soils at this site. The closed canopy assumptions built into the model conceptualize the canopy as being spread out over the landscape, rather than being composed of patches of vegetation and patches of open soil. For open-canopy systems, a two-component model that accounts for the surface area covered by vegetation, and a separate component that accounts for bare soil, would likely be more effective [*Norman et al.*, 1995; *Van den Hurk and McNaughton*, 1995].

3.3. Flux Variation With Meteorological Conditions

[35] Variation in soybean (Figure 10) F_c with R_g indicates that light saturation commences at lower R_g (around 400 [W m^{-2}]), or earlier in the day, relative to the response of maize (Figure 11). This is due to both leaf- and canopy-scale factors. Soybean leaves saturate faster, at lower incident *PAR* flux densities, than do maize leaves. The soybean canopy is also generally denser, with much of that foliage concentrated in the upper third of the canopy space. This reduces the radiation use efficiency of the canopy by inhibiting radiation penetration to light-limited foliage in the lower canopy, pointing to the potential for the modification of canopy architecture as a method to improve soybean photosynthesis [*Long et al.*, 2006a]. The mean response of maize F_c to R_g is linear until the shortwave forcing reaches approximately 800 [W m^{-2}], at which point the response levels off due to light saturation of the foliage at the canopy top.

[36] Maize energy fluxes maintain the linear increase through the entire range of R_g, indicating that energy partitioning between *LE* and *H* remains constant on average through the course of the day. *LE* and *H* for the soybean canopy increase linearly with R_g, with greater partitioning of energy to *H* at the highest R_g values due in part to the effect of saturating A_n on g_s [*Ball et al.*, 1987]. Some of the increase in F_c and increase in energy partitioned to *H* is also due to the covariation of R_g and *VPD* under water stress conditions (discussed below).

[37] The temperature response of both canopies is flat for each flux until T_a approaches 20°C, at which point a sharp increase in CO_2 uptake and latent heat flux occurs, as higher temperature values correspond to daytime conditions. The flux responses plateau at the highest temperatures, as these conditions correspond to light saturation conditions discussed above. Sensible heat flux increase flattens for both soybean and maize as T_a approaches 30°C, where the energy requirements to increase T_l above the ambient air temperature

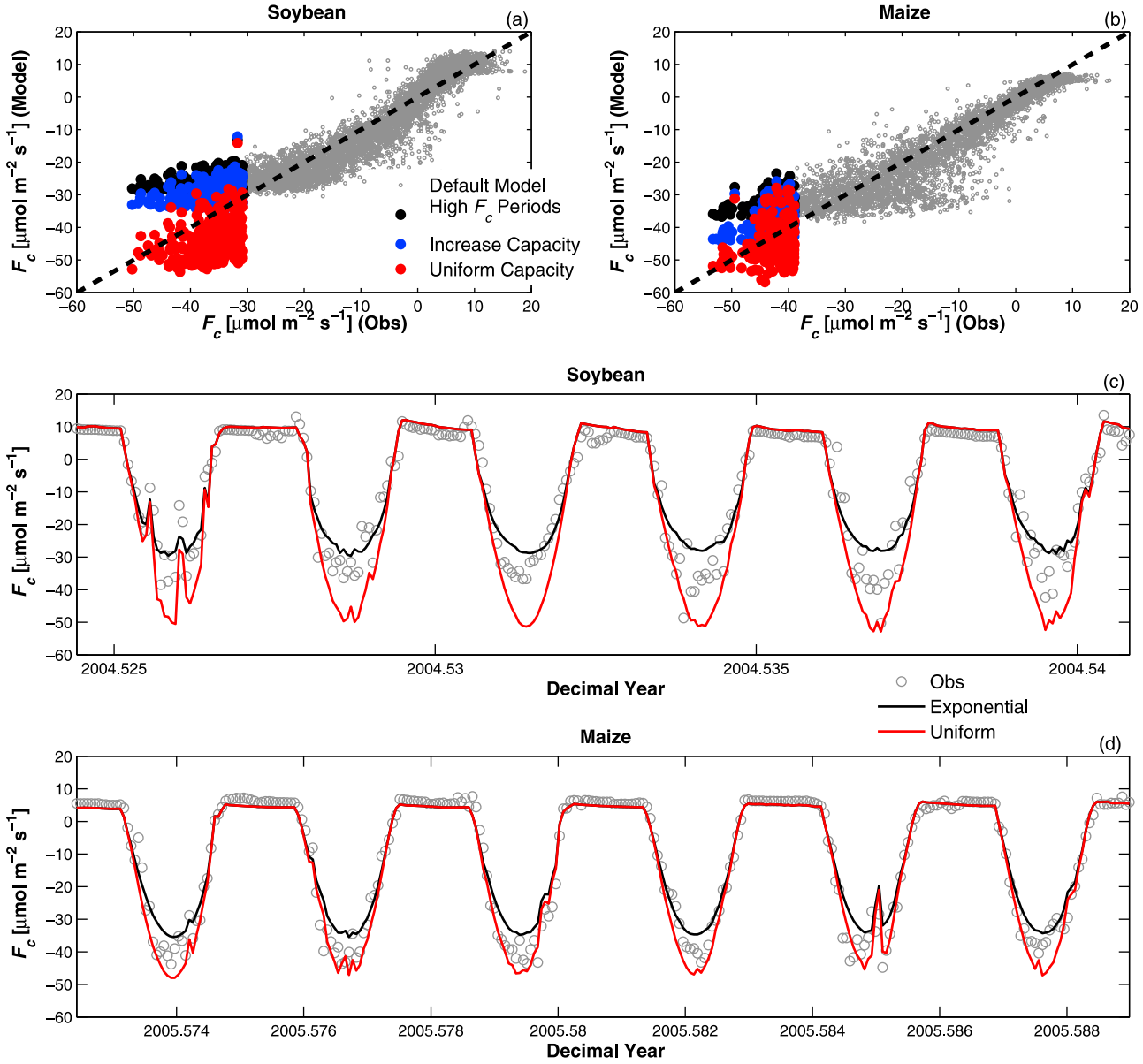

Figure 9. Sensitivity analysis of the effects of photosynthetic capacity on peak flux estimates. (a and b) The model F_c predictions with default parameter values against those observed are presented as gray dots. Black dots represent observed fluxes that were greater in magnitude than predictions. Blue and red dots demonstrate the effect of increases in photosynthetic capacity and allowing photosynthetic capacity to be uniform through the canopy. Six days in (c) 2004 and (d) 2005 are shown, in which peak observed flux values (gray dots) were underestimated by the default model (black lines), along with estimates made with uniform photosynthetic capacity through the canopy (red lines).

are nullified in part by greater longwave emission. Soybean H appears to be slightly underestimated by the model for the highest air temperatures, but in general the variations in the three observed fluxes to T_a are well replicated for both crops.

[38] The observed response to *VPD* is curvilinear for soybean F_c and *LE* (Figure 10). The initial increase in CO_2 uptake and vapor release slows and then reverses at the highest *VPD* values experienced over the three study years. The initial increase of CO_2 and vapor exchange with *VPD* is due to the covariation of R_g and *VPD* over the course of a typical day. Relative humidity declines as *VPD* increases, resulting in stomatal closure (see equation (11) in Text S1) and the plateau of CO_2 and vapor exchange seen in Figure 10. A sharp increase in H is seen to occur at the highest *VPD* values, indicating a change in energy partitioning for *VPD* values >1.6 [kPa]. These periods of high *VPD* correspond to periods of plant water stress, with *LAD*-weighted Ψ_l equal to −0.7 [MPa] during these periods, relative to an average value of −0.2 [MPa] over all simulated periods. Reductions in Ψ_l result in a canopy-averaged reduction in stomatal conductance of 14% for these dry periods (see Figure 4c), with as high as a 42% loss of stomatal conductance at localized regions within the canopy. This is in addition to the stomatal closure induced by the reduction in h_s at leaf surfaces as *VPD*

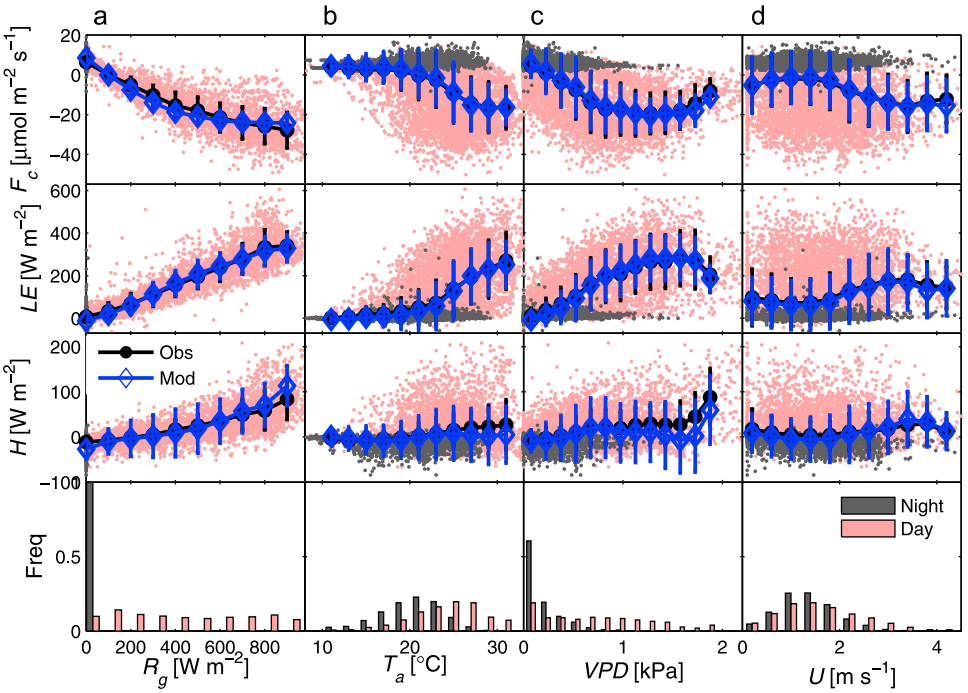

Figure 10. Relationship between modeled and observed net canopy-atmosphere fluxes of CO_2, latent energy, and sensible heat fluxes and environmental conditions for soybean. Variation with respect to (a) downward shortwave, (b) air temperature, (c) vapor pressure deficit, and (d) wind speed are presented for observed fluxes (black dots/lines) and modeled fluxes (blue dots/lines), with vertical bars representing ± one standard deviation. Half-hourly daytime observations are presented as red dots, and nighttime observations are presented as black dots.

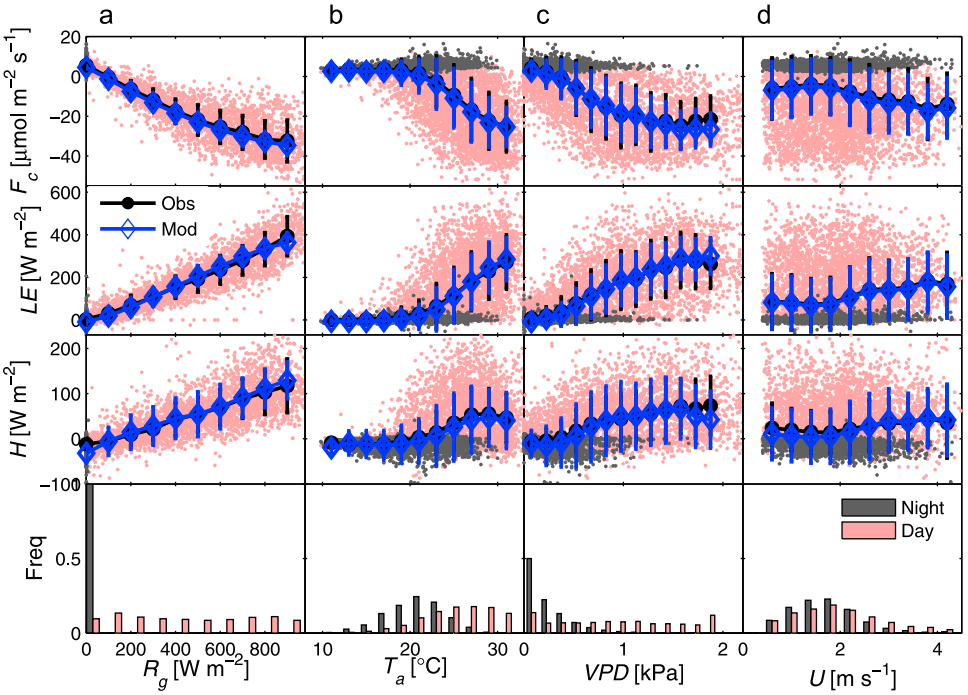

Figure 11. Same as Figure 10 for maize.

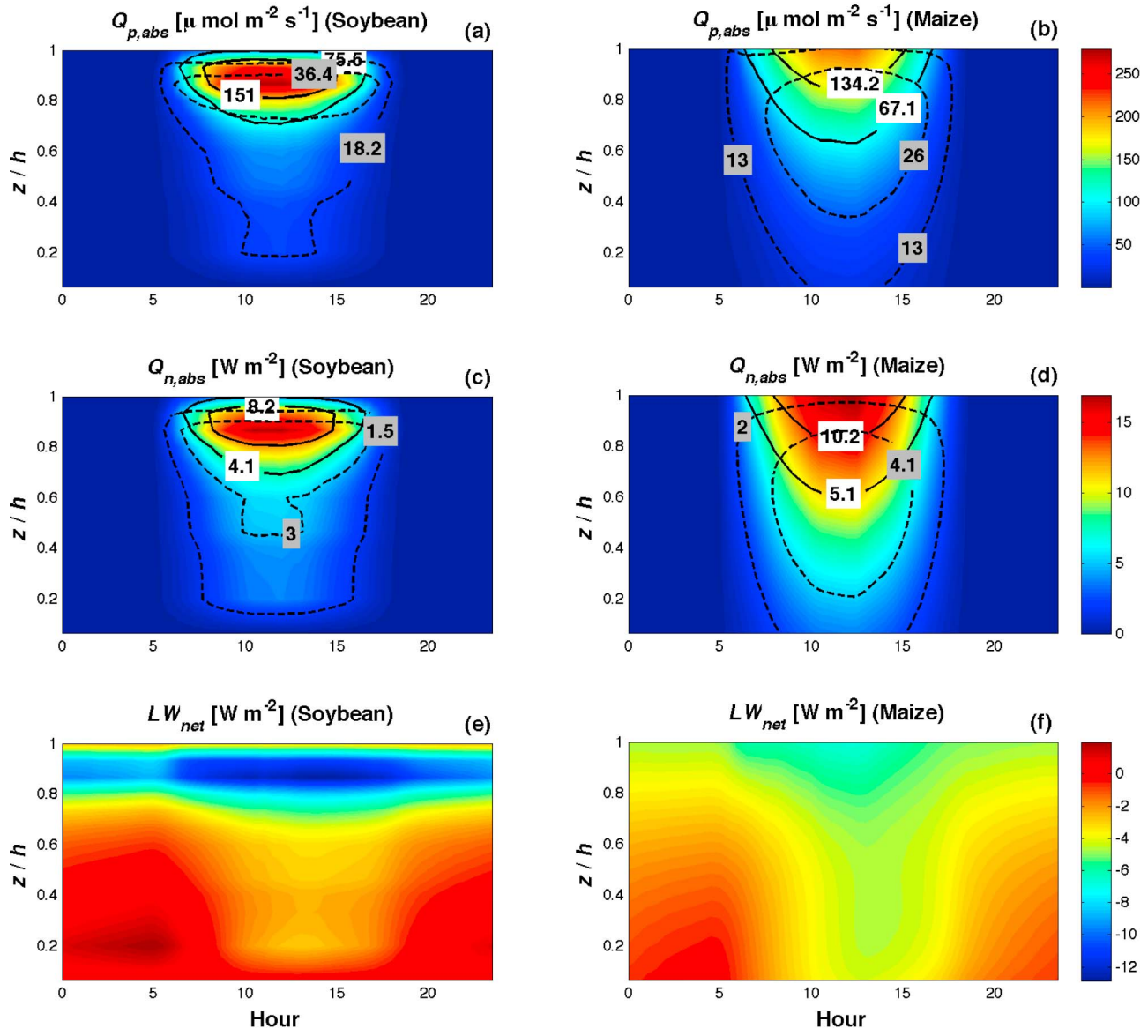

Figure 12. Diurnally averaged canopy profiles of (a and b) absorbed *PAR* ($Q_{p,abs}$), (c and d) absorbed *NIR* ($Q_{n,abs}$), and (e and f) net longwave radiation (LW_{net}) for (left) soybean and (right) maize. Solid black lines represent flux contours for the sunlit canopy fraction. Dashed black lines represent flux contours for the shaded canopy fraction. The same color scales are used for identical fluxes for both canopies to facilitate direct comparison.

increases. Similar, but less dramatic, modification to energy partitioning can be seen for maize (Figure 11), with an average reduction in g_s of 10% for these periods. Only a slight reduction in F_c occurs for maize, as C4 metabolism is much less sensitive to reductions in g_s, except for extreme stomatal closure, as indicated by the dashed arrow in Figure 2. The model shows good general agreement with the trends in each flux with *VPD*, with a slight oversensitivity to high *VPD* (moisture stress) for maize and a minor undersensitivity for soybean, which may be explained by uncertainties in the specification of the relationship depicted in Figure 4c.

[39] Each of the three fluxes shows an increase in magnitude with increasing U, as R_g and U are usually positively correlated. Higher wind speeds result in larger boundary layer conductances, particularly in the upper portion of the canopies where CO_2 and water vapor exchange are greatest, resulting in higher C_a and lower e_a at the leaf surfaces.

3.4. Vertical Variation of Canopy Radiation Regime

[40] The shortwave radiation incident on a foliage layer is the principle driver of CO_2, vapor and heat exchange through its control on photosynthesis and leaf energy balance (see Figure 2). In Figure 12, the influence of canopy structure is apparent when contrasting the absorbed radiation profiles between soybean and maize. The soybean *LAD* profile is characterized by several local maxima, with the largest peak in leaf area at $z/h \simeq 0.85$ for the 1 m tall canopy (see Figure 4).

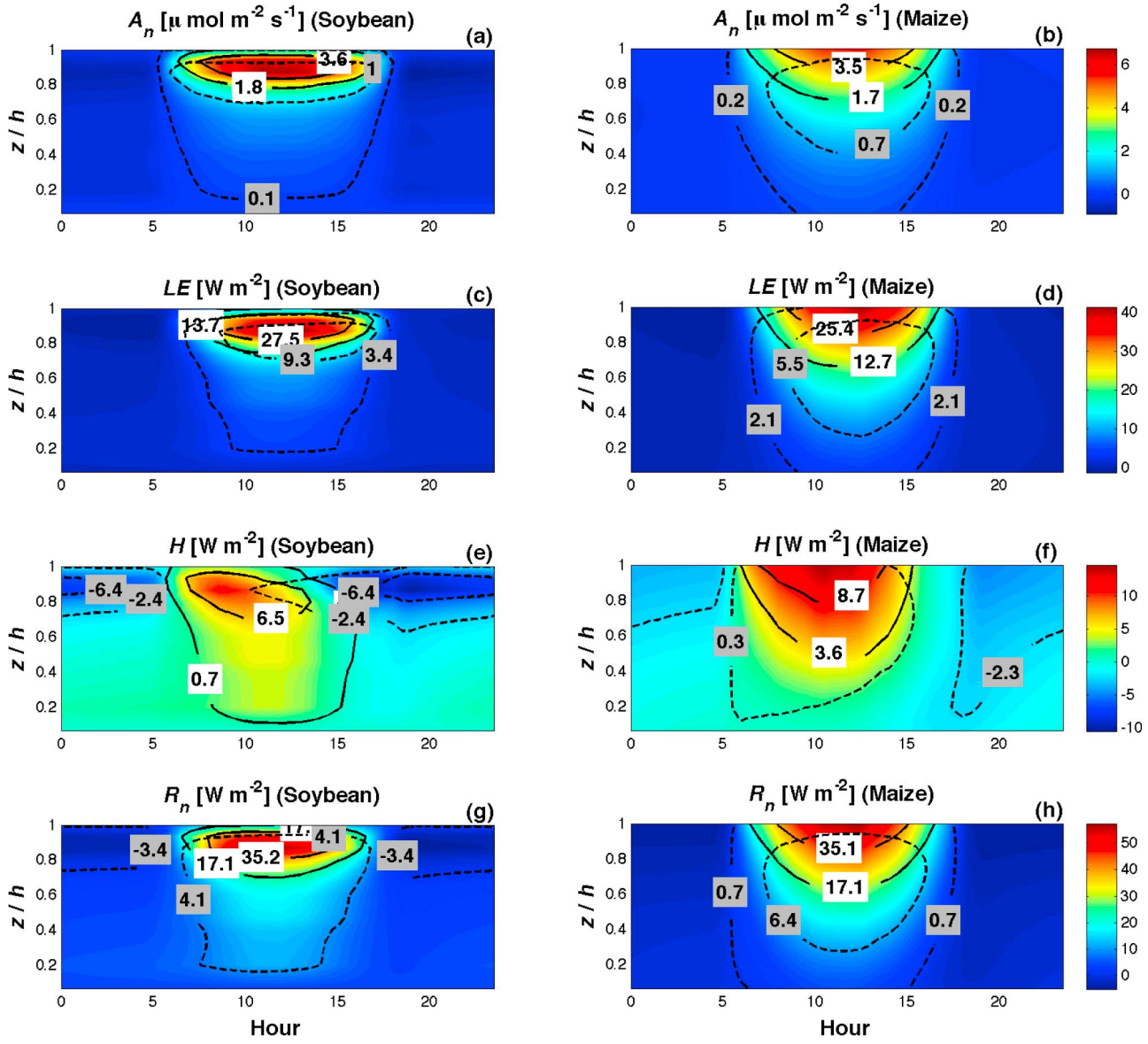

Figure 13. Diurnally averaged (a and b) net CO_2, (c and d) latent heat, (e and f) sensible heat, and (g and h) net radiation flux profiles for (left) soybean and (right) maize. Solid black lines represent flux contours for the sunlit canopy fraction. Dashed black lines represent flux contours for the shaded canopy fraction. The same color scales are used for identical fluxes for both canopies to facilitate direct comparison.

The high soybean *LAI* values (mean ≃5 over all study periods) result in dense foliage at this level that dominates radiation absorption for the entire range of sun angles experienced during the day. The combination of high *PAR* absorptivity and the dense peak in *LAD* result in the absorption or reflection out of the system of most of the *PAR* by $z/h = 0.7$. At 1200 local time, the top one fourth of the canopy absorbs approximately 52% of the *PAR* (Figure 12a) and 45% of the *NIR* (Figure 12c) absorbed by the entire canopy. This results in a highly localized CO_2 (energy) sink (source) region at the top of the canopy (see Figure 13), with much of the foliage below this *LAD* peak making a minor contribution to scalar exchange.

[41] In contrast, the maize canopy *LAD* profile is more uniform, with the peak values located between $z/h = 0.5$ and 0.7 and each node of the 15-layer canopy comprising 5 to 7.5% of the total *LAI*. The more uniform *LAD* profile, and slightly less dense canopy (mean *LAI* values ≃4.1 over all study periods), results in greater absorption deeper in the canopy by the sunlit fraction and the 33% contour for the shaded fraction extending to the bottom of the canopy. At 1200 local time, the three canopy layers spanning the peak in maize *LAD* absorb ~30% of the *PAR* (Figure 12b) and 14% of the *NIR* (Figure 12d) absorbed by the entire canopy. *NIR* absorption is distributed deeper in both canopies due to the much lower leaf absorptivity for *NIR*, resulting in a much higher contribution of the shaded fraction to the total canopy *NIR* absorption.

[42] The dense upper portion of the soybean canopy is a net source of longwave energy throughout the average diurnal

cycle (Figures 12e and 12f), with the maximum outgoing longwave occurring during daylight hours when the canopy is receiving the most intense shortwave forcing, raising T_l and longwave emission. The maize canopy LW_{net} is more uniformly distributed vertically through the canopy due to the more uniform shortwave forcing.

[43] The influence of the vertical canopy structures of soybean and maize are evident in the distributions of shortwave radiation, the primary forcing of CO_2 and energy exchange, through the canopy. The impacts of these structural differences on flux magnitudes are presented in section 3.5.

3.5. Vertical Variation in Canopy-Atmosphere Exchange

[44] Canopy-atmosphere exchange of carbon dioxide, water vapor and heat is strongly dependent on the magnitude of R_g incident on the foliage. Foliage distributions and leaf radiative properties determine how the radiation incident at the canopy-top penetrates through the canopy, exciting scalar sources/sinks. Here we follow the investigation of the vertical patterns of absorbed radiation through the canopy in section 3.4 with an examination of the patterns of soybean and maize scalar flux densities. The diurnal distributions of A_n and *LE* for soybean (Figures 13a and 13c) and maize (Figure 13b and 13d) correspond closely to the patterns of *PAR* and *NIR* seen in Figure 12, as *PAR* is the primary driver of A_n and absorbed shortwave radiation (SW_{abs}) provides the majority of the energy partitioned into *LE* and *H*.

[45] A_n and *LE* for soybean are localized around the upper canopy local maximum, while the fluxes for maize occur more uniformly through the upper half of the canopy with greater relative contributions deeper in the canopy. The top 30% of the soybean canopy is responsible for 80% of the canopy A_n and 70% of canopy *LE* at noon, in contrast to 66% of canopy A_n and 59% of canopy *LE* for maize. This upper portion of the canopy accounts for 90% of the sunlit and 60% of the shaded soybean A_n, relative to 82% of the sunlit and 48% of the shaded canopy *LE* for maize, where the deeper penetration of *NIR* results in a greater proportion of *LE* in the lower canopy.

[46] A greater fraction of available energy is partitioned to *LE* for soybean as opposed to maize, as can be seen by comparing the *LE* and *H* (Figures 13e and 13f) panels for the two canopies. Most of the energy exchange by the soybean canopy occurs around the upper canopy local maximum, where the majority of shortwave flux is absorbed, as can be seen from the diurnal variation in R_n (Figure 13g). The R_n patterns are a function of the distribution of *H* and *LE* as well as the net longwave flux through the canopy, calculated here as the difference between absorbed and emitted radiation components.

[47] A higher contribution of *H* from the lower portion of the soybean canopy, where photosynthesis is not active, is apparent in the R_n panel. The *H* contours indicate that the sunlit canopy fraction is the primary contributor to sensible heat flux to the atmosphere by the soybean canopy. Positive *H* is distributed more deeply in the soybean canopy than the more highly localized upper canopy carbon dioxide sink, due to the ability of *NIR* to penetrate the dense upper soybean canopy. The maize canopy also displays greater lower-canopy relative sensible heat flux contributions. The maize shaded canopy fraction is a source of sensible heat to the atmosphere as the more uniform and less dense canopy allows more diffuse radiation, both *PAR* (as indicated in Figure 13b) and *NIR*, to penetrate deeper. The upper canopy is a sink of sensible heat at night for both canopies, somewhat offset at the canopy scale by a small positive heat flux in the lower canopy levels which have a positive LW_{net} at night (see Figure 12) due to absorption of the soil longwave emission.

[48] The less localized distributions of absorbed shortwave and A_n for maize result in more uniform increases in g_s with smaller magnitudes than the highly active upper canopy of soybean. This allows T_l to rise through the maize canopy, forcing more available energy to be dissipated as sensible, rather than latent heat, reducing canopy water loss and resulting in greater water use efficiency.

3.6. Water Stress Impacts

[49] Here we examine the role of the subsurface moisture regime in modulating canopy-atmosphere exchange for the two crops. In addition to the simulations conducted to validate the model, a second set of simulations were performed for each crop in which the hydraulic constraint on stomatal conductance was removed, making g_s completely insensitive to root zone moisture availability. These will be referred to as the "No Hydraulic Constraint," or NoHC, simulations, in contrast to the fully coupled canopy-root-soil (HC) simulations. The NoHC case leaves only A_n and environmental factors to affect g_s and the partitioning of energy between latent and sensible heating, essentially removing the dependence of g_s on soil moisture status, by way of Ψ_l as depicted in Figure 4c, that is incorporated into the fully coupled model.

[50] The final seven days of the 18 day simulation period shown in Figures 14a–14c indicate the onset of moisture stress and the effect of the hydraulic constraint, beginning 11 days after a rain event during the night of DOY 206. A modification in the partitioning of energy, away from *LE* toward *H*, becomes more pronounced over this period for the HC case. This is the result of stomatal closure induced by decreases in root zone soil moisture in the upper 0.75 m of the soil column where the majority of the root biomass resides. Figures 14e and 14f show the simulated soil moisture through the soil column for HC, and the root pressure potential (Ψ_r) through the root zone for HC, respectively (Figure 14f). Reductions in θ result in decreasing Ψ_r and consequently Ψ_l, forcing stomatal closure by way of the dependence of g_s on Ψ_l depicted in Figure 4c [*Jones*, 1992; *Lhomme*, 1998; *Tuzet et al.*, 2003]. The change in energy partitioning is greater than 100 [W m^{-2}] during midday and late afternoon periods of several of the days experiencing moisture stress. Despite the large changes in energy partitioning experienced during this period, only a slight reduction in the magnitude of F_c is apparent at the end of the period, potentially a result of metabolic limitations due to moisture stress [*Vico and Porporato*, 2008].

[51] The daytime ($R_g > 50$ [W m^{-2}]) water use efficiency (*WUE*), calculated as the total daytime A_n divided by total daytime *LE*, is presented in Figure 14d, where T_r is transpiration. Here *WUE* accounts only for canopy fluxes, eliminating potential biases induced through the effects of soil fluxes. As available soil moisture decreases, the *WUE* of the HC case becomes greater than that of the NoHC case. Recent observational work has demonstrated leaf- and plant-level increases in *WUE* of water-stressed crops under controlled

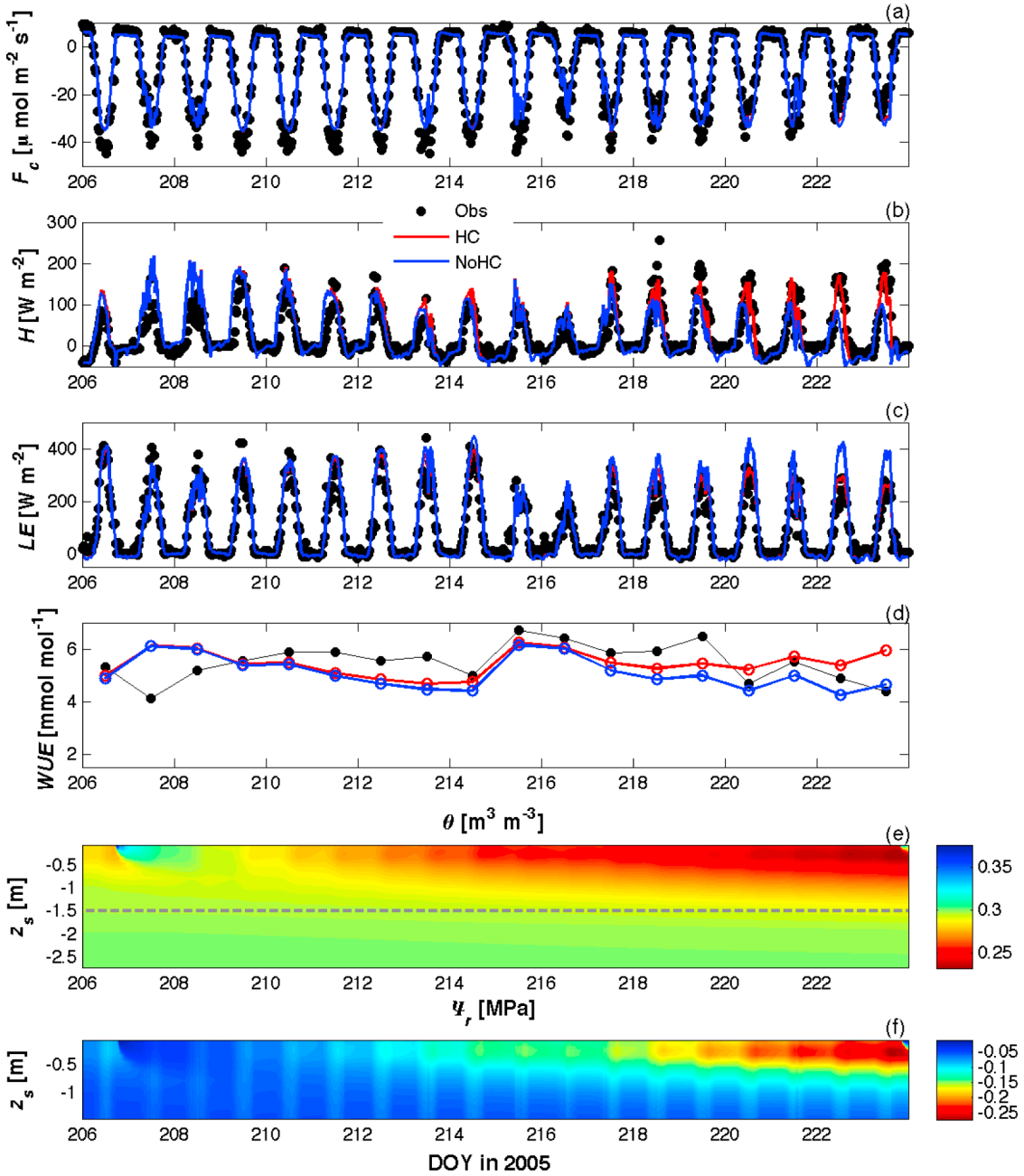

Figure 14. Demonstration of the effects of water stress for maize during an 18 day period in 2005. Diurnal records of observed (black dots), modeled (blue lines), and modeled without hydraulic control (red lines) fluxes over an 18 day period in 2005 for maize. (a) Net CO_2 flux, (b) latent energy flux, (c) sensible heat flux, and (d) water use efficiency. (e) Soil moisture through the modeled soil column with the depth of the root zone denoted by a dashed gray line, and (f) root pressure potential through the root zone.

conditions [*Chen et al.*, 1993; *Liu et al.*, 2005], but left open the question of how the complete canopy would respond to moisture stress in an uncontrolled environment. Canopy behavior can significantly differ from that of single leaves under a given set of environmental conditions [*Baldocchi et al.*, 1985]. Likewise, plant responses in the open field often diverge from those in controlled environments [*Long et al.*, 2006b]. Previous studies conducted in open-field conditions concluded that canopy *WUE* decreases as moisture stress increases [*Sinclair et al.*, 1975; *Baldocchi et al.*, 1985]. The micrometeorological techniques applied in these studies, however, were not able to differentiate soil changes from those of the canopy.

[52] As stress increases (f_{sv} decreases), stomatal closure occurs at the canopy top and progresses downward into the canopy (contours in Figures 15b and 15d). The greatest effects on A_n, *LE*, and *H* (not shown) occur in the region of densest foliage for the soybean canopy, where most of the gas

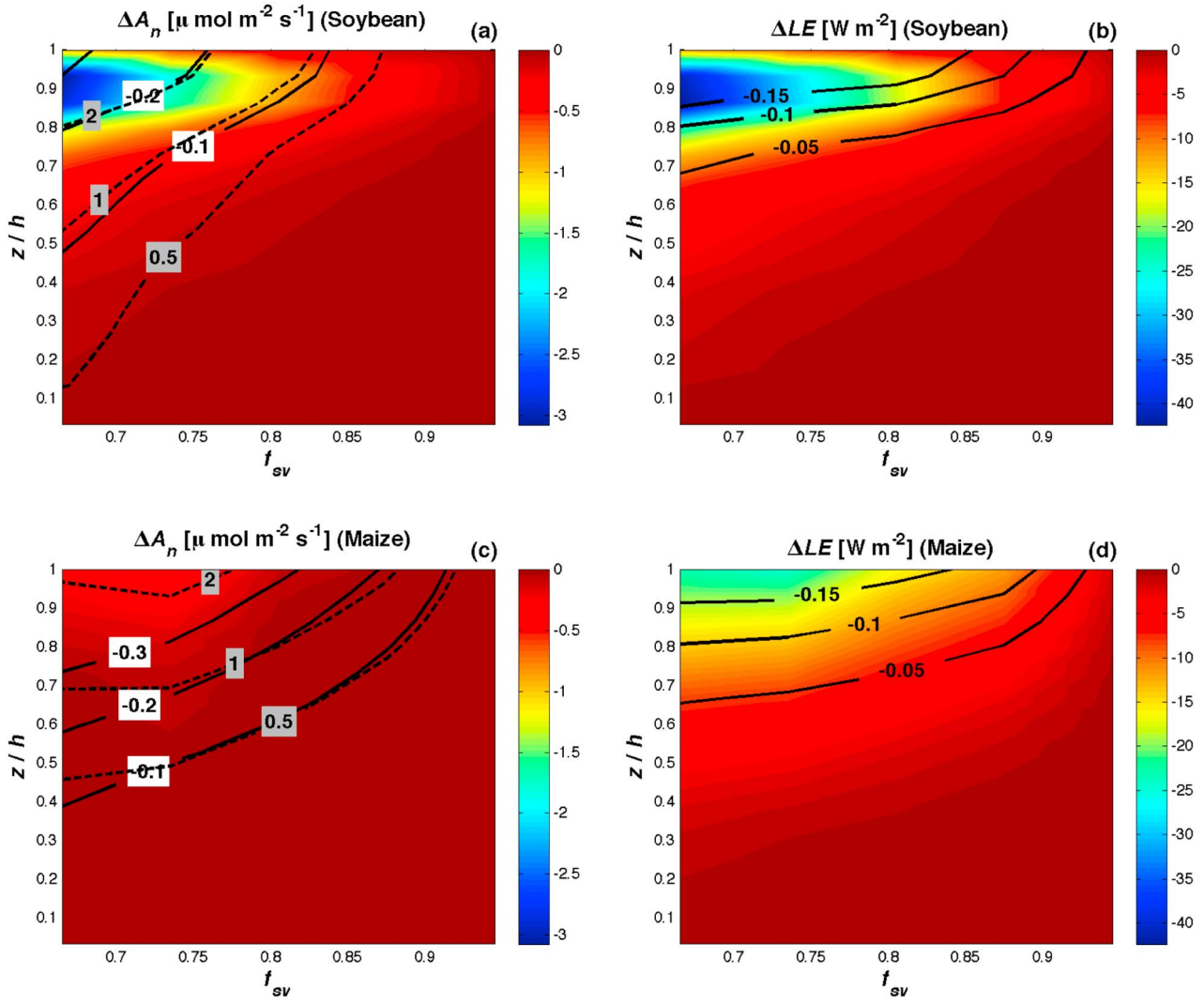

Figure 15. Average differences (Δ) in flux profiles (HC-NoHC), binned according to the canopy-averaged reduction in stomatal conductance (f_{sv}). (a and c) The Δ in net CO_2 flux through the soybean and maize canopies. Black contours represent changes in C_i/C_a, and gray contours represent changes in T_l. (b and d) The changes (HC-NoHC) in latent energy exchange through the soybean and maize canopies. Black contours here represent changes in g_s.

exchange is occurring. The vertical patterns of gas exchange in the maize canopy are governed primarily by radiation absorption rather than by local maxima in *LAD* (see Figure 13). The more uniform maize canopy therefore shows reductions in flux that more closely follow the pattern of reduction of g_s from the canopy top, progressing downward as stress increases. The patterns of the reductions in *LE* are identical to those of the increases in *H* (not shown), while the magnitude of the increase in *H* is less than that of the reductions in *LE* due to the greater longwave dissipation as T_l increases. Maize A_n shows considerable resilience to moisture stress relative to the soybean canopy, due to the insensitivity of A_n to C_i, as controlled by g_s, resulting from the CO_2 concentrating mechanism of C4 biochemistry.

[53] As mean canopy stomatal closure approaches 35%, mean canopy A_n of soybean is reduced by 40% and *LE* is reduced by 50% (Figure 16). The reduction in A_n increases nonlinearly, relative to the near-linear decrease in *LE*, due to the nonlinear response of A_n to C_i which makes photosynthesis more sensitive to variations in C_i as it decreases. This results in the flattening of the increase in ΔWUE as stress increases, over the range of canopy stress examined here, at approximately 0.6 [mmol mol^{-1}], or 17%. Maize A_n shows only minor reductions to moisture stress, with mean canopy *LE* reduced as much as 150 [W m^{-2}]. This results in an approximately linear increase in *WUE* as the maize canopy experiences greater moisture stress, up to a 45% increase as mean canopy stomatal closure approaches 65%. Water stress therefore has the effect of further enhancing the difference in water use efficiency between the more water use efficient C4 maize canopy and that of the C3 soybean canopy.

[54] The results presented in this section demonstrate the significant effect of moisture stress on the functioning of both C3 and C4 crop species, with canopy structure and

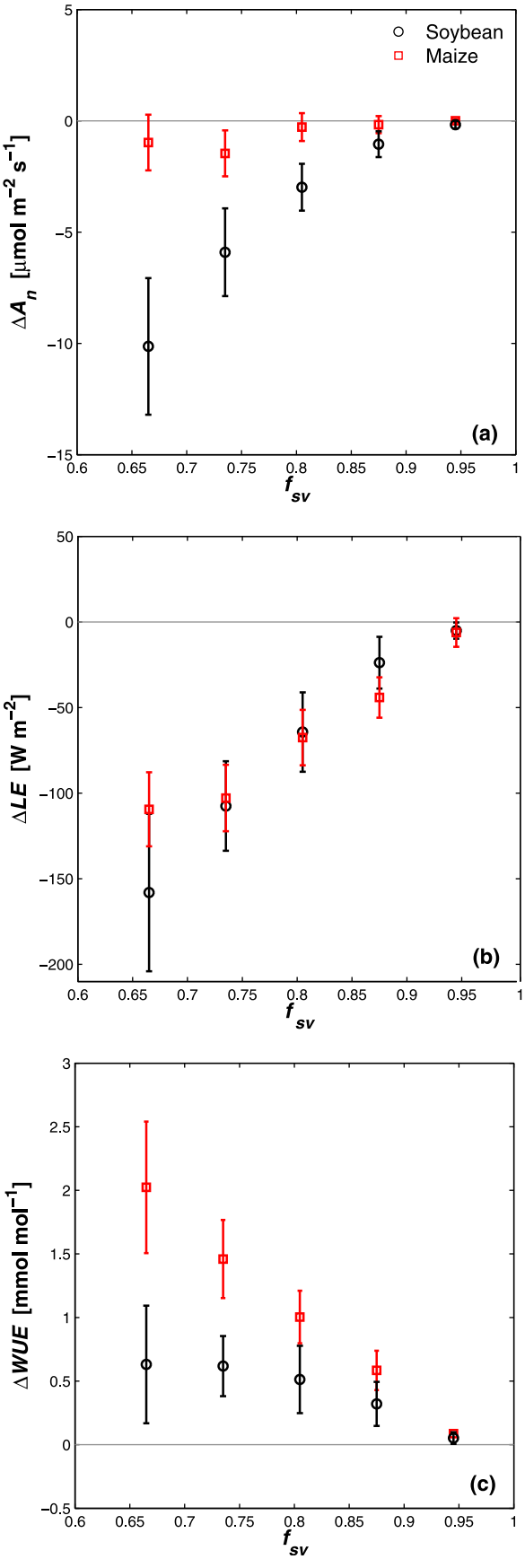

ecophysiology each playing a role in the net canopy response. The large shift in canopy energy partitioning from latent to sensible heat fluxes for field-grown soybean and maize has the potential to impact the interactions between central U.S. agriculture and atmospheric boundary layer dynamics that govern the environment experienced at the land surface. In an enriched CO_2 environment, in which plants are generally more water conservative due to the widely observed reduction in stomatal aperture, these effects may be partially mitigated. The companion paper [*Drewry et al.*, 2010] utilizes the MLCan framework presented here to analyze canopy-scale responses to elevated CO_2 concentrations projected over the coming century.

4. Summary and Conclusion

[55] This paper addressed the role of structural and ecophysiological properties of two important crop species, soybean and maize, on canopy-atmosphere exchange of carbon dioxide, water vapor and energy. The analysis is conducted using a new synthesis of coupled canopy, leaf, root and soil processes resolved vertically through the canopy and soil domains (MLCan). MLCan has been designed to allow flexibility in the choice of photosynthetic type, C3 or C4, while maintaining consistency in the model formulation, providing a platform that can be used to evaluate the role of photosynthetic metabolism on ecosystem processes across a wide range of climate regimes. Using data from 7488 and 6192 half-hour periods collected over three growing seasons each for the soybean and maize canopies, respectively, at the Bondville Ameriflux site, MLCan flux estimates demonstrated good agreement with observed canopy-top CO_2, latent and sensible heat fluxes over a wide range of meteorological conditions.

[56] An examination of the variations in canopy-atmosphere exchange as a function of meteorological forcing demonstrated a saturation in F_c by the soybean canopy as R_g increased. The resolved radiation absorption profiles showed this to be due to the dense light-saturated upper canopy foliage capturing radiation that could potentially be more efficiently used in the shaded, light-limited lower canopy. The more uniformly distributed foliage of the maize canopy resulted in near linear increases in F_c, LE and H with rising R_g. The control of moisture stress on energy partitioning, observed during high VPD conditions, which were correlated with periods of low soil moisture, resulted in the reduction in soybean CO_2 uptake and greater dissipation of energy by sensible heat for both canopies. Soybean experienced a reversal in the trends of increasing carbon gain and latent energy fluxes as VPD increased beyond 1.6 [kPa]. The model captured this canopy-integrated behavior through the coupling between canopy physics, ecophysiology, biochemistry and subsurface moisture dynamics.

[57] The roles of canopy structure and photosynthetic metabolism on the vertical patterns of hydraulic control of gas exchange were examined through the canopies of each crop.

Figure 16. Net changes (HC-NoHC) in canopy-atmosphere exchange of (a) CO_2, (b) latent heat, and (c) WUE for soybean (black symbols) and maize (red symbols) as a function of the fraction of canopy mean stomatal conductance not lost due to hydraulic limitation.

The dense upper canopy soybean foliage resulted in major changes in canopy carbon and energy exchange being localized to this region. Maize foliage was more uniformly distributed through the canopy domain, resulting in changes in fluxes that were higher at the canopy top and followed more closely the pattern of change in stomatal conductance through the canopy. Maize A_n was more resilient to moisture stress relative to soybean which showed a progressive reduction in A_n as moisture stress became more severe. Both canopies demonstrated significant changes in net energy partitioning from *LE* to *H* as stress increased, with a mean canopy stomatal closure of 35% resulting in shifts from *LE* to *H* greater than 100 [W m^2] for both canopies. The combined effects of moisture stress on A_n and *LE* produced a limitation in increased *WUE* by soybean approaching 20%, whereas maize *WUE* increased linearly through the range of moisture stress examined in this study up to approximately 45%. Overall, the results demonstrate the potentially significant effect of moisture stress on the functioning of these C3 and C4 crops, with canopy structure and ecophysiology each playing a role in the net canopy responses. These modifications in energy partitioning by the two most common Midwestern U.S. agricultural species could have significant implications for large-scale interactions of the vegetated land surface with the atmospheric boundary layer. The potential for reduced summer rainfall in the central United States as a consequence of projected future climate variability [*Wuebbles and Hayhoe*, 2004] necessitate a better understanding of the large-scale effects of crop stress.

[58] **Acknowledgments.** This research is primarily funded by NSF grant ATM 06-28687 and partially supported by NOAA grant NA 06-OAR4310053. We wish to thank the PIs of the Bondville Fluxnet tower and the FACE experimental facility. Benjamin Burroughs conducted valuable data synthesis work that is gratefully acknowledged. Insightful comments of Lisa Ainsworth and Andrew Leakey helped shape some initial thinking on this project. Juan Quijano, Venkat Srinivasan, and Phong Le provided valuable comments on early versions of the manuscript. We also thank the Editor (Dennis Baldocchi) and an Associate Editor for *JGR-Biogeosciences*, along with two anonymous reviewers, whose insightful comments greatly improved the manuscript.

References

Ainsworth, E. A., and S. P. Long (2005), What have we learned from 15 years of free-air CO_2 enrichment (FACE)? A meta-analytic review of the responses of photosynthesis, canopy properties and plant production to rising CO_2, *New Phytol.*, *165*(2), 351–372.

Albertson, J., G. Katul, and P. Wiberg (2001), Relative importance of local and regional controls on coupled water, carbon, and energy fluxes, *Adv. Water Resour.*, *24*(9–10), 1103–1118.

Amenu, G., and P. Kumar (2008), A model for hydraulic redistribution incorporating coupled soil-root moisture transport, *Hydrol. Earth Syst. Sci.*, *12*(1), 55–74.

Amthor, J. (1994), Scaling CO_2-photosynthesis relationships from the leaf to the canopy, *Photosynth. Res.*, *39*(3), 321–350.

Anderson, M. P., J. M. Norman, T. P. Meyers, and G. R. Diak (2000), An analytical model for estimating canopy transpiration and carbon assimilation fluxes based on canopy light-use efficiency, *Agric. For. Meteorol.*, *101*(4), 265–289.

Baldocchi, D., and P. Harley (1995), Scaling carbon dioxide and water vapour exchange from leaf to canopy in a deciduous forest. ii. model testing and application, *Plant Cell Environ.*, *18*(10), 1157–1173.

Baldocchi, D., and T. Meyers (1998), On using eco-physiological, micrometeorological and biogeochemical theory to evaluate carbon dioxide, water vapor and trace gas fluxes over vegetation: A perspective, *Agric. For. Meteorol.*, *90*(1–2), 1–25.

Baldocchi, D., S. Verma, and N. Rosenberg (1985), Water use efficiency in a soybean field: Influence of plant water stress, *Agric. For. Meteorol.*, *34*(1), 53–65.

Baldocchi, D., K. Wilson, and L. Gu (2002), How the environment, canopy structure and canopy physiological functioning influence carbon, water and energy fluxes of a temperate broad-leaved deciduous forest-An assessment with the biophysical model CANOAK, *Tree Physiol.*, *22*(15–16), 1065.

Ball, J., I. Woodrow, and J. Berry (1987), A model predicting stomatal conductance and its contribution to the control of photosynthesis under different environmental conditions, in *Progress in Photosynthesis Research*, vol. 4, edited by J. Biggins, pp. 221–224, Martinus Nijhoff, Dordrecht, Netherlands.

Bernacchi, C., C. Pimentel, and S. Long (2003), In vivo temperature response functions of parameters required to model RuBP-limited photosynthesis, *Plant Cell Environ.*, *26*(9), 1419–1430.

Bernacchi, C., P. Morgan, D. Ort, and S. Long (2005a), The growth of soybean under free air CO_2 enrichment (FACE) stimulates photosynthesis while decreasing in vivo rubisco capacity, *Planta*, *220*(3), 434–446.

Bernacchi, C., S. Hollinger, and T. Meyers (2005b), The conversion of the corn/soybean ecosystem to no-till agriculture may result in a carbon sink, *Global Change Biol.*, *11*(11), 1867–1872.

Bernacchi, C., B. Kimball, D. Quarles, S. Long, and D. Ort (2007), Decreases in stomatal conductance of soybean under open-air elevation of [CO_2] are closely coupled with decreases in ecosystem evapotranspiration, *Plant Physiol.*, *143*(1), 134–144.

Blizzard, W., and J. Boyer (1980), Comparative resistance of the soil and the plant to water transport, *Plant Physiol.*, *66*(5), 809–814.

Boedhram, N., T. Arkebauer, and W. Batchelor (2001), Season-long characterization of vertical distribution of leaf area in corn, *Agron. J.*, *93*(6), 1235–1242.

Brisson, N., A. Olioso, and P. Clastre (1993), Daily transpiration of field soybeans as related to hydraulic conductance, root distribution, soil potential and midday leaf potential, *Plant Soil*, *154*(2), 227–237.

Brutsaert, W. (1982), *Evaporation Into The Atmosphere: Theory, History and Applications*, Springer, New York.

Bunce, J. (2004), Carbon dioxide effects on stomatal responses to the environment and water use by crops under field conditions, *Oecologia*, *140*(1), 1–10.

Caldwell, M., H. Meister, J. Tenhunen, and O. Lange (1986), Canopy structure, light microclimate and leaf gas exchange of Quercus coccifera L. in a Portuguese macchia: Measurements in different canopy layers and simulations with a canopy model, *Trees Structure Function*, *1*(1), 25–41.

Campbell, G. S., and J. M. Norman (1998), *Introduction to Environmental Biophysics*, 2nd ed., edited by G. S. Campbell and J. M. Norman, Springer, New York.

Chen, X., G. Begonia, D. Alm, and J. Hesketh (1993), Responses of soybean leaf photosynthesis to CO_2 and drought, *Photosynthetica*, *29*(3), 447–454.

Collatz, G., M. Ribas-Carbo, and J. Berry (1992), Coupled physiological-stomatal conductance model for leaves C4 plants, *Aust. J. Plant Physiol.*, *19*(5), 519–538.

Curtis, P. (1996), A meta-analysis of leaf gas exchange and nitrogen in trees grown under elevated carbon dioxide, *Plant Cell Environ.*, *19*(2), 127–137.

Davidson, E., I. Janssens, and Y. Luo (2006), On the variability of respiration in terrestrial ecosystems: Moving beyond Q10, *Global Change Biol.*, *12*(2), 154–164.

Dermody, O., S. Long, and E. DeLucia (2006), How does elevated CO_2 or ozone affect the leaf-area index of soybean when applied independently?, *New Phytol.*, *169*(1), 145–155.

Drewry, D. T., P. Kumar, S. Long, C. Bernacchi, X.-Z. Liang, and M. Sivapalan (2010), Ecohydrological responses of dense canopies to environmental variability: 2. Role of acclimation under elevated CO_2, *J. Geophys. Res.*, *115*, G04023, doi:10.1029/2010JG001341.

Ellsworth, D. (2000), Seasonal CO_2 assimilation and stomatal limitations in a pinus taeda canopy, *Tree Physiol.*, *20*(7), 435.

Ellsworth, D., and P. Reich (1993), Canopy structure and vertical patterns of photosynthesis and related leaf traits in a deciduous forest, *Oecologia*, *96*(2), 169–178.

Feddes, R., et al. (2001), Modeling root water uptake in hydrological and climate models, *Bull. Am. Meteorol. Soc.*, *82*(12), 2797–2809.

Field, C. (1983), Allocating leaf nitrogen for the maximization of carbon gain: Leaf age as a control on the allocation program, *Oecologia*, *56*(2), 341–347.

Furbank, R., C. Jenkins, and M. Hatch (1989), CO_2 concentrating mechanism of C4 photosynthesis permeability of isolated bundle sheath cells to inorganic carbon, *Plant Physiol.*, *91*(4), 1364–1371.

Gedney, N., P. Cox, R. Betts, O. Boucher, C. Huntingford, and P. Stott (2006), Detection of a direct carbon dioxide effect in continental river runoff records, *Nature*, *439*(7078), 835–838.

Ghannoum, O. (2009), C4 photosynthesis and water stress, *Ann. Bot.*, *103*(4), 635–644.

Goudriaan, J. (1977), Crop micrometeorology: A simulation study, Cent. for Agric. Publ. and Doc., Wageningen, Netherlands.

Goulden, M., J. Munger, S. Fan, B. Daube, and S. Wofsy (1996), Measurements of carbon sequestration by long-term eddy covariance: Methods and a critical evaluation of accuracy, *Global Change Biol.*, *2*(3), 169–182.

Gu, L., H. Shugart, J. Fuentes, T. Black, and S. Shewchuk (1999), Micrometeorology, biophysical exchanges and NEE decomposition in a two-story boreal forest: Development and test of an integrated model, *Agric. For. Meteorol.*, *94*, 123–148.

Gutschick, V. P. (2007), Plant acclimation to elevated CO_2: From simple regularities to biogeographic chaos, *Ecol. Modell.*, *200*(3–4), 433–451.

Hatch, M. (1987), C4 photosynthesis: A unique blend of modified biochemistry, anatomy and ultrastructure, *Biochim. Biophys. Acta*, *895*(8), 1–106.

Hinzman, L., D. Goering, and D. Kane (1998), A distributed thermal model for calculating soil temperature profiles and depth of thaw in permafrost regions, *J. Geophys. Res.*, *103*(D22), 28,975–28,991.

Hollinger, S., C. Bernacchi, and T. Meyers (2005), Carbon budget of mature no-till ecosystem in North Central Region of the United States, *Agric. For. Meteorol.*, *130*(1–2), 59–69.

Horn, H. (1971), *The Adaptive Geometry of Trees*, Princeton Univ. Press, Princeton, N. J.

Huang, B., and P. Nobel (1994), Root hydraulic conductivity and its components, with emphasis on desert succulents, *Agron. J.*, *86*(5), 767.

Huxman, T., E. Hamerlynck, B. Moore, S. Smith, D. Jordan, S. Zitzer, R. Nowak, J. Coleman, and J. Seemann (1998), Photosynthetic down-regulation in Larrea tridentata exposed to elevated atmospheric CO_2: Interaction with drought under glasshouse and field(FACE) exposure, *Plant Cell Environ.*, *21*(11), 1153–1161.

Jackson, R., H. Mooney, and E. Schulze (1997), A global budget for fine root biomass, surface area, and nutrient contents, *Proc. Natl. Acad. Sci.*, *94*(14), 7362.

Jackson, R., et al. (2000), Belowground consequences of vegetation change and their treatment in models, *Ecol. Appl.*, *10*(2), 470–483.

Janssens, I., and K. Pilegaard (2003), Large seasonal changes in Q10 of soil respiration in a beech forest, *Global Change Biol.*, *9*(6), 911–918.

Jones, H. (1973), Moderate-term water stresses and associated changes in some photosynthetic parameters in cotton, *New Phytol.*, *72*, 1095–1105.

Jones, H. (1992), *Plants and Microclimate: A Quantitative Approach to Environmental Plant Physiology*, Cambridge Univ. Press, New York.

Kabela, E., B. Hornbuckle, M. Cosh, M. Anderson, and M. Gleason (2009), Dew frequency, duration, amount, and distribution in corn and soybean during smex05, *Agric. For. Meteorol.*, *149*(1), 11–24.

Katul, G., L. Mahrt, D. Poggi, and C. Sanz (2004), One-and two-equation models for canopy turbulence, *Boundary Layer Meteorol.*, *113*(1), 81–109.

Kleidon, A., and M. Heimann (2000), Assessing the role of deep rooted vegetation in the climate system with model simulations: Mechanism, comparison to observations and implications for Amazonian deforestation, *Clim. Dyn.*, *16*(2), 183–199.

Labat, D., Y. Goddéris, J. L. Probst, and J. L. Guyot (2004), Evidence for global runoff increase related to climate warming, *Adv. Water Resour.*, *27*(6), 631–642.

Lai, C., G. Katul, D. Ellsworth, and R. Oren (2000), Modelling vegetation-atmosphere CO_2 exchange by a coupled Eulerian-Langrangian approach, *Boundary Layer Meteorol.*, *95*(1), 91–122.

Lang, A. (1991), Application of some of Cauchy's theorems to estimation of surface areas of leaves, needles and branches of plants, and light transmittance, *Agric. For. Meteorol.*, *55*(3–4), 191–212.

Lavigne, M., et al. (1997), Comparing nocturnal eddy covariance measurements to estimates of ecosystem respiration made by scaling chamber measurements at six coniferous boreal sites, *J. Geophys. Res.*, *102*(D24), 28,977–28,985.

Leakey, A., C. Bernacchi, D. Ort, and S. Long (2006a), Photosynthesis, productivity, and yield of maize are not affected by open-air elevation of CO_2 concentration in the absence of drought 1 [oa], *Plant Cell Environ.*, *29*(9), 1794–1800.

Leakey, A., M. Uribelarrea, E. Ainsworth, S. Naidu, A. Rogers, D. Ort, and S. Long (2006b), Photosynthesis, productivity, and yield of maize are not affected by open-air elevation of CO_2 concentration in the absence of drought 1 [oa], *Plant Physiol.*, *140*(2), 779–790.

Leuning, R., F. Kelliher, D. Pury, and E. Schulze (1995), Leaf nitrogen, photosynthesis, conductance and transpiration: Scaling from leaves to canopies, *Plant Cell Environ.*, *18*(10), 1183–1200.

Lhomme, J. (1998), Formulation of root water uptake in a multi-layer soil-plant model: Does van den Honert's equation hold?, *Hydrol. Earth Syst. Sci.*, *2*, 31–40.

Liu, F., M. Andersen, S. Jacobsen, and C. Jensen (2005), Stomatal control and water use efficiency of soybean (Glycine max L. Merr.) during progressive soil drying, *Environ. Exp. Bot.*, *54*(1), 33–40.

Long, S. P., E. A. Ainsworth, A. Rogers, and D. R. Ort (2004), Rising atmospheric carbon dioxide: Plants FACE the future, *Ann. Rev. Plant Biol.*, *55*(1), 591–628.

Long, S., X. Zhu, S. Naidu, and D. Ort (2006a), Can improvement in photosynthesis increase crop yields?, *Plant Cell Environ.*, *29*(3), 315–30.

Long, S. P., E. A. Ainsworth, A. D. B. Leakey, J. Nosberger, and D. R. Ort (2006b), Food for thought: Lower-than-expected crop yield stimulation with rising CO_2 concentrations, *Science*, *312*(5782), 1918–1921.

Massman, W., and X. Lee (2002), Eddy covariance flux corrections and uncertainties in long-term studies of carbon and energy exchanges, *Agric. For. Meteorol.*, *113*(1–4), 121–144.

Meyers, T., and S. Hollinger (2004), An assessment of storage terms in the surface energy balance of maize and soybean, *Agric. For. Meteorol.*, *125*(1–2), 105–115.

Meyers, T., M. Heuer, and T. Wilson (2010), Ameriflux bondville site description, Oak Ridge Natl. Lab., Oak Ridge, Tenn. (Available at http://public.ornl.gov/ameriflux/)

Midgley, J. (2003), Is bigger better in plants? The hydraulic costs of increasing size in trees, *Trends Ecol. Evol.*, *18*(1), 5–6.

Moncrieff, J., Y. Malhi, and R. Leuning (1996), The propagation of errors in long-term measurements of land-atmosphere fluxes of carbon and water, *Global Change Biol.*, *2*(3), 231–240.

Morgan, P., G. Bollero, R. Nelson, F. Dohleman, and S. Long (2005), Smaller than predicted increase in aboveground net primary production and yield of field-grown soybean under fully open-air [CO_2] elevation, *Global Change Biol.*, *11*(10), 1856–1865.

Nikolov, N., and K. Zeller (2003), Modeling coupled interactions of carbon, water, and ozone exchange between terrestrial ecosystems and the atmosphere. i: Model description, *Environ. Pollut.*, *124*(2), 231–246.

Nikolov, N., W. Massman, and A. Schoettle (1995), Coupling biochemical and biophysical processes at the leaf level: An equilibrium photosynthesis model for leaves of c3 plants, *Ecol. Modell.*, *80*(2–3), 205–235.

Norman, J. (1979), Modeling the complete crop canopy, in *Modification of the Aerial Environment of Crops*, pp. 249–280, Am. Soc. of Agric. Eng., St. Joseph, Mich.

Norman, J., W. Kustas, and K. Humes (1995), Source approach for estimating soil and vegetation energy fluxes in observations of directional radiometric surface temperature, *Agric. For. Meteorol.*, *77*(3–4), 263–293.

Oleson, K., et al. (2004), Technical description of the community land model (CLM), *Tech. Note NCAR/TN-461+ STR*, Natl. Cent. for Atmos. Res., Boulder, Colo.

Ort, D., E. Ainsworth, M. Aldea, D. Allen, C. Bernacchi, M. Berenbaum, and G. Bollero (2006), SoyFACE: The effects and interactions of elevated [CO_2] and [O3] on soybean, in *Managed Ecosystems and CO_2: Case Studies, Processes, and Perspectives*, pp. 71–85, Springer, New York.

Palmroth, S., C. Maier, H. McCarthy, A. Oishi, H. Kim, K. Johnsen, G. Katul, and R. Oren (2005), Contrasting responses to drought of forest floor CO_2 efflux in a Loblolly pine plantation and a nearby Oak-Hickory forest, *Global Change Biol.*, *11*(3), 421–434.

Poggi, D., A. Porporato, L. Ridolfi, J. Albertson, and G. Katul (2004), The effect of vegetation density on canopy sub-layer turbulence, *Boundary Layer Meteorol.*, *111*(3), 565–587.

Pyles, R., B. Weare, and K. Pawu (2000), The UCD advanced canopy-atmosphere-soil algorithm: Comparisons with observations from different climate and vegetation regimes, *Q. J. R. Meteorol. Soc.*, *126*(569), 2951–2980.

Raupach, M. (1989), Applying Lagrangian fluid mechanics to infer scalar source distributions from concentration profiles in plant canopies, *Agric. For. Meteorol.*, *47*(2–4), 85–108.

Sage, R. (1994), Acclimation of photosynthesis to increasing atmospheric CO_2: The gas exchange perspective, *Photosynth. Res.*, *39*(3), 351–368.

Sage, R., T. Sharkey, and J. Seemann (1989), Acclimation of photosynthesis to elevated CO_2 in five C3 species 1, *Plant Physiol.*, *89*(2), 590–596.

Schenk, H., and R. Jackson (2002), The global biogeography of roots, *Ecol. Monogr.*, *72*(3), 311–328.

Schulze, E., and A. Hall (1982), Stomatal responses, water loss and CO_2 assimilation rates of plants in contrasting environments, *Encycl. Plant Physiol.*, *12*, 181–230.

Sinclair, T., G. Bingham, E. Lemon, and L. Allen Jr. (1975), Water use efficiency of field-grown maize during moisture stress, *Plant Physiol.*, *56*(2), 245.

Sinclair, T., C. Murphy, and K. Knoerr (1976), Development and evaluation of simplified models for simulating canopy photosynthesis and transpiration, *J. Appl. Ecol.*, *13*(3), 813–829.

Siqueira, M., G. Katul, and A. Porporato (2008), Onset of water stress, hysteresis in plant conductance, and hydraulic lift: Scaling soil water dynamics from millimeters to meters, *Water Resour. Res.*, *44*, W01432, doi:10.1029/2007WR006094.

Sperry, J. (2000), Hydraulic constraints on plant gas exchange, *Agric. For. Meteorol.*, *104*(1), 13–23.

Spitters, C. (1986), Separating the diffuse and direct component of global radiation and its implications for modeling canopy photosynthesis. II: Calculation of canopy photosynthesis, *Agric. For. Meteorol.*, *38*(1–3), 231–242.

Tufekcioglu, A., J. Raich, T. Isenhart, and R. Schultz (1998), Fine root dynamics, coarse root biomass, root distribution, and soil respiration in a multispecies riparian buffer in Central Iowa, USA, *Agrofor. Syst.*, *44*(2), 163–174.

Tuzet, A., A. Perrier, and R. Leuning (2003), A coupled model of stomatal conductance, photosynthesis and transpiration, *Plant Cell Environ.*, *26*(7), 1097–1116.

Tyree, M., and J. Sperry (1988), Do woody plants operate near the point of catastrophic xylem dysfunction caused by dynamic water stress? 1 Answers from a model, *Plant Physiol.*, *88*(3), 574–580.

Van den Hurk, B., and K. McNaughton (1995), Implementation of near-field dispersion in a simple two-layer surface resistance model, *J. Hydrol.*, *166*(3–4), 293–311.

Vico, G., and A. Porporato (2008), Modelling C3 and C4 photosynthesis under water-stressed conditions, *Plant Soil*, *313*(1), 187–203.

von Caemmerer, S., and R. Furbank (1999), Modeling C4 photosynthesis, in *C4 Plant Biology*, edited by R. Sage and R. Monson, pp. 173–211, Academic, San Diego, Calif.

Weiss, A., D. Lukens, J. Norman, and J. Steadman (1989), Leaf wetness in dry beans under semi-arid conditions, *Agric. For. Meteorol.*, *48*(1–2), 149–162.

Welles, J., and J. Norman (1991), Instrument for indirect measurement of canopy architecture, *Agron. J.*, *83*(5), 818.

Williams, M., E. Rastetter, D. Fernandes, M. Goulden, S. Wofsy, G. Shaver, J. Melillo, J. Munger, S. Fan, and K. Nadelhoffer (1996), Modelling the soil-plant-atmosphere continuum in a Quercus-Acer stand at Harvard Forest: The regulation of stomatal conductance by light, nitrogen and soil/plant hydraulic properties, *Plant Cell Environ.*, *19*(8), 911–927.

Wilson, K., and T. Meyers (2001), The spatial variability of energy and carbon dioxide fluxes at the floor of a deciduous forest, *Boundary Layer Meteorol.*, *98*(3), 443–473.

Wilson, K., D. Baldocchi, and P. Hanson (2000a), Spatial and seasonal variability of photosynthetic parameters and their relationship to leaf nitrogen in a deciduous forest, *Tree Physiol.*, *20*(9), 565–578.

Wilson, K., D. Baldocchi, and P. Hanson (2000b), Quantifying stomatal and non-stomatal limitations to carbon assimilation resulting from leaf aging and drought in mature deciduous tree species, *Tree Physiol.*, *20*(12), 787.

Wu, J., Y. Liu, and D. Jelinski (2000), Effects of leaf area profiles and canopy stratification on simulated energy fluxes: The problem of vertical spatial scale, *Ecol. Modell.*, *134*(2), 283–297.

Wuebbles, D., and K. Hayhoe (2004), Climate change projections for the United States Midwest, *Mitig. Adapt. Strateg. Global Change*, *9*(4), 335–363.

Xu, L., and D. Baldocchi (2003), Seasonal trends in photosynthetic parameters and stomatal conductance of blue oak (quercus douglasii) under prolonged summer drought and high temperature, *Tree Physiol.*, *23*(13), 865.

C. Bernacchi, Department of Plant Biology, University of Illinois, Urbana, IL 61801, USA.

D. T. Drewry, Max Planck Institute for Biogeochemistry, D-07745 Jena, Germany.

P. Kumar and M. Sivapalan, Department of Civil and Environmental Engineering, University of Illinois, Urbana, IL 61801, USA. (kumar1@illinois.edu)

X.-Z. Liang, Illinois State Water Survey, Champaign, IL 61820, USA.

S. Long, Department of Crop Sciences, University of Illinois, Urbana, IL 61801, USA.